International Journal for Parasitology: Drugs and Drug Resistance 19 (2022) 65–80

Contents lists available at ScienceDirect

International Journal for Parasitology: Drugs and Drug Resistance

journal homepage: www.elsevier.com/locate/ijpddr

Insights from the use of erythropoietin in experimental Chagas disease

Ana Carolina de Castro Nobre [a], Carlos Fernando Pimentel [a], George Magno Sousa do Rêgo [b], Giane Regina Paludo [b], Glaucia Bueno Pereira Neto [c], Márcio Botelho de Castro [d], Nadjar Nitz [a], Mariana Hecht [a], Bruno Dallago [a,c], Luciana Hagström [a,e,*]

[a] Interdisciplinary Laboratory of Biosciences, Faculty of Medicine, University of Brasilia, Brasília, Brazil
[b] Laboratory of Veterinary Clinical Pathology, Faculty of Agronomy and Veterinary Medicine, University of Brasília, Brasília, Brazil
[c] Veterinary Hospital, Faculty of Agronomy and Veterinary Medicine, University of Brasília, Brasília, Brazil
[d] Laboratory of Veterinary Pathology, Faculty of Agronomy and Veterinary Medicine, University of Brasília, Brasília, Brazil
[e] Faculty of Physical Education, University of Brasília, Brasília, Brazil

ARTICLE INFO

Keywords:
Trypanosoma cruzi
Therapeutic drug
Erythropoietin
Cardioprotection
Mice

ABSTRACT

In addition to the long-established role in erythropoiesis, erythropoietin (Epo) has protective functions in a variety of tissues, including the heart. This is the most affected organ in chronic Chagas disease, caused by the protozoan *Trypanosoma cruzi*. Despite seven million people being infected with *T. cruzi* worldwide, there is no effective treatment preventing the disease progression to the chronic phase when the pathological involvement of the heart is often observed. Chronic chagasic cardiomyopathy has a wide variety of manifestations, like left ventricular systolic dysfunction, dilated cardiomyopathy, and heart failure. Since Epo may help maintain cardiac function by reducing myocardial necrosis, inflammation, and fibrosis, this study aimed to evaluate whether the Epo has positive effects on experimental Chagas disease. For that, we assessed the earlier (acute phase) and also the later (chronic phase) use of Epo in infected C57BL/6 mice. Blood cell count, biochemical parameters, parasitic load, and echocardiography data were evaluated. In addition, histopathological analysis was carried out. Our data showed that Epo had no trypanocide effect nor did it modify the production of anti-*T. cruzi* antibodies. Epo-treated groups exhibited parasitic burden much lower in the heart compared to blood. No pattern of hematological changes was observed combining infection with treatment with Epo. Chronic Epo administration reduced CK-MB serum activity from d0 to d180, irrespectively of *T. cruzi* infection. Likewise, echocardiography and histological results indicate that Epo treatment is more effective in the chronic phase of experimental Chagas disease. Since treatment is one of the greatest challenges of Chagas disease, alternative therapies should be investigated, including Epo combined with benznidazole.

1. Introduction

Chagas disease, caused by the protozoan *Trypanosoma cruzi*, is an endemic disease in Latin America. Due to globalization and population migration, the disease has been spread and become a global health problem. It has been estimated that seven million people are infected with *T. cruzi* worldwide (WHO, 2019).

The hallmark of the acute phase of Chagas disease, which lasts two months in humans, is the high parasitic burden. This stage is usually asymptomatic or presents mild non-specific symptoms (Bern, 2015). In a few cases, it can be observed cardiac impairment as myocarditis with myocytolytic necrosis and heart failure (Bern, 2015; Coura and Borges-Pereira, 2010). In this phase, cardiac involvement is mostly observed in orally transmitted *T. cruzi* infection (Franco-Paredes et al., 2020), in which cardiomegaly has been seen (Dias et al., 2008; Pinto et al., 2004, 2008).

The acute infection is followed by the low parasitemia chronic phase. This stage can remain asymptomatic for several years, however, 20–30% of infected people develop cardiac and/or digestive complications decades after the initial infection (Bern, 2015; Prata, 2001).

Chagas chronic cardiomyopathy is the most serious clinical manifestation and the main cause of lethality (Bocchi et al., 2017; Cunha-Neto and Chevillard, 2014). The disease manifests in different ways being able to progress to heart failure and cardiac arrest. Patients might

* Corresponding author. Interdisciplinary Laboratory of Biosciences, Faculty of Medicine, Campus Darcy Ribeiro. University of Brasilia, 70910-900, Brasília, Distrito Federal, Brazil.
E-mail addresses: hagstrom@unb.br, loubex@hotmail.com (L. Hagström).

https://doi.org/10.1016/j.ijpddr.2022.05.005
Received 27 August 2021; Received in revised form 26 May 2022; Accepted 31 May 2022
Available online 17 June 2022

have several heart alterations such as arrhythmias, syncope, and left ventricular dysfunction (Bern, 2015). The main histopathological findings are diffuse myocarditis with infiltration of mononuclear inflammatory cells, myocytolysis, and fibrosis (Parada et al., 1997; Teixeira et al., 2011).

Only two drugs are available as a therapeutic option for Chagas disease (nifurtimox and benznidazole) and their effectiveness is far from ideal (Pérez-Molina et al., 2021). While in the acute Chagas disease the treatment can achieve cure in up to 76% of patients (Cançado, 2002), the efficacy in the chronic phase is uncertain (Santacruz et al., 2021) and is not correlated with a better outcome (Cevey et al., 2017; Morillo et al., 2015). Cevey et al., for example, showed that treatment with benznidazole for 15 consecutive days during the chronic phase did not improve the left ventricular function in mice (Cevey et al., 2017). Thus, the need for improving current therapy, developing new medicines, or finding alternative drugs for Chagas disease are critical issues (Ribeiro et al., 2020). The use of medicaments approved and available in the pharmaceutical market for the treatment of other diseases (i.e. repositioning of existing therapeutic drugs) is considered an effective, low-cost, and riskless strategy since its safety has already been proven (Xue et al., 2018). In this study, we chose to test an erythropoietin (Epo) analogue as a treatment for *T. cruzi* infections.

Epo is a glycoprotein produced mainly by the kidneys in adult mammals. Its main function is the promotion of proliferation and terminal differentiation of erythroid progenitor cells resulting in increased production of red blood cells (RBC) (for review, see Suresh et al., 2020). From observations that Epo and his receptor (EpoR) are expressed in different tissues, such as the brain (Marti, 2004; Wakhloo et al., 2020), skeletal muscles (Hagström et al., 2010; Launay et al., 2010), and heart (El Hasnaoui-Saadani et al., 2013; Puchulu et al., 2019; Smith et al., 2003; Tramontano et al., 2003; Wright et al., 2004) the functions of this cytokine have been extended beyond erythropoiesis (Suresh et al., 2020). Several studies have shown cardioprotection conferred by the administration of Epo (for review, see Riksen et al., 2008; Sanchis-Gomar et al., 2014) through an antiapoptotic effect (Latini et al., 2008; Qin et al., 2013), mobilization of progenitor cells from the bone marrow, as well as an anti-hypertrophic action (Latini et al., 2008) and reduction in inflammation (Burger et al., 2009; Qin et al., 2013). It has been suggested that Epo may reverse cardiac remodeling in some conditions as mouse heart failure (Li et al., 2006). This action preserves ventricular function. Besides, Epo promotes angiogenesis in the heart (Burger et al., 2009; Lu et al., 2012).

Since Epo has important physiological and clinical implications (Lombardero et al., 2011; Moore et al., 2011; Suresh et al., 2020) with proven cardioprotection performance, it arises as a promising alternative for the treatment of *T. cruzi* infections. We hypothesized that Epo will not affect the parasite (no trypanocide capacity), but will protect the infected heart due to its antiapoptotic and anti-inflammatory well-known actions despite its angiogenic effect which may increase the levels of circulating parasites in the heart due to the neovascularization, as well as pro-inflammatory molecules.

Thus, this study aims to evaluate whether Epo exerts cardioprotective effects on the experimental Chagas disease. The treatment took place during the acute phase since this period may influence the disease outcome and during the chronic phase, the period in which serious cardiac complications can arise.

2. Material and methods

2.1. Animal model

Female C57BL/6 mice aged 30–35 days and weighting 16.61 ± 2.20 g, obtained from Multidisciplinary Center for Biological Research in the Area of Science in Laboratory Animals (CEMIB/UNICAMP, São Paulo, Brazil) were used in the experiments. The mice were housed in standard conditions (temperature 20–23 °C under 12/12 h light/dark cycle with free access to tap water and commercial food). The experimental procedure was performed in agreement with the National Council for Animal Experimentation Control (CONCEA) and was approved by the Ethical Committee on Animal Experimentation of the University of Brasília (CEUA/UnB, protocol number nº150813/2014).

2.2. Experimental infection and parasitemia evaluation

The myotropic Colombian strain (genotype TcI) (Zingales et al., 2009) was maintained by two passages of blood form trypomastigotes in C57BL/6 mice every 30 days. The animals of infected groups were intraperitoneally inoculated with 5×10^5 trypomastigotes/mL on day 1 (d1). Controls mice received saline alone. The presence of *T. cruzi* in mice peripheral blood was evaluated by microscopic examination of blood smear seven days after infection according to the methodology described by Brenner (Brener, 1962). This procedure was repeated daily until confirmation of infection.

2.3. Experimental groups

Aiming to evaluate the possible therapeutic effect of Epo in Chagas disease, mice were treated in the acute or the chronic phase of *T. cruzi* infection. The infection lasted 180 days for all mice. In this way, mice were treated with intraperitoneal (i.p.) injections of 2,000 IU/kg of recombinant human Epo (Hemax Eritron alfaEpoetina, Biosintética Farmacêutica) given on alternate days starting either on the first day post-inoculation (dpi) with *T. cruzi* or on 90th dpi. The treatment lasted 30 days, with 15 Epo doses in total. Infected control mice receive i.p. saline solution (NaCl 0.9%) (vehicle) only. Uninfected mice received Epo or saline on the equivalent periods.

Mice were divided randomly into eight groups. The first four groups were composed of animals who received Epo or saline during the acute phase (AP) of *T. cruzi* infection (or in equivalent period for uninfected groups). The animals were distributed into the following groups: (1) Infected with *T. cruzi* and treated with Epo from 1 dpi to 30 dpi (d1 to d30) (I_Epo_AP); (2) Infected-untreated who received saline from d1 to d30 (I_S_AP); (3) Uninfected treated with Epo between the first experimental day (d1) and the 30th day (d30) (NI_Epo_AP) and (4) Uninfected-untreated who received saline between d1 and d30 (NI_S_AP) (Fig. 1A).

The other four groups received Epo or saline during the chronic phase (CP) of *T. cruzi* infection (or in equivalent period for uninfected mice). The animals were distributed as follows: (5) Infected with *T. cruzi* and treated with Epo from 90 dpi to 120 dpi (d90 to d120) (I_Epo_CP); (6) Infected-untreated who received saline from d90 to d120 (I_S_CP); (7) Uninfected treated with Epo between 90th experimental day (d90) and the 120th day (d120) (NI_Epo_CP) and (8) Uninfected-untreated who received saline between d90 and d120 (NI_S_CP) (Fig. 1A).

2.4. Hematological evaluation

The day before the beginning of Epo or saline administration and at the end of the time of each treatment (30 dpi or 120 dpi) the packed cell volume or hematocrit (Hct) was measured. For that, mice were i.p. anesthetized with ketamine hydrochloride 10% and xylazine hydrochloride 2% based on their body weight (2:1; maximal dose 10 mL/kg) (Syntec) and blood from orbital sinus was collected in heparinized capillary microtubes. Hct was obtained by the microhematocrit method using a microcentrifuge (MH 11.5i, Inbras).

At baseline (d0) and immediately before the euthanasia (d180) blood samples were collected as described above. Complete blood count (CBC) was performed and hemoglobin concentration (HGB) was determined using an automatic cell counter (ABX® Micros ESV 60, Horiba). Hct was determined by the microhematocrit method. Whole blood smears were prepared and stained with Diff-Quick (Instant Prov, Newprov, Brazil) for leukocyte differential count. The smears were analyzed by light microscopy and at least 100 white blood cells (WBC) were counted.

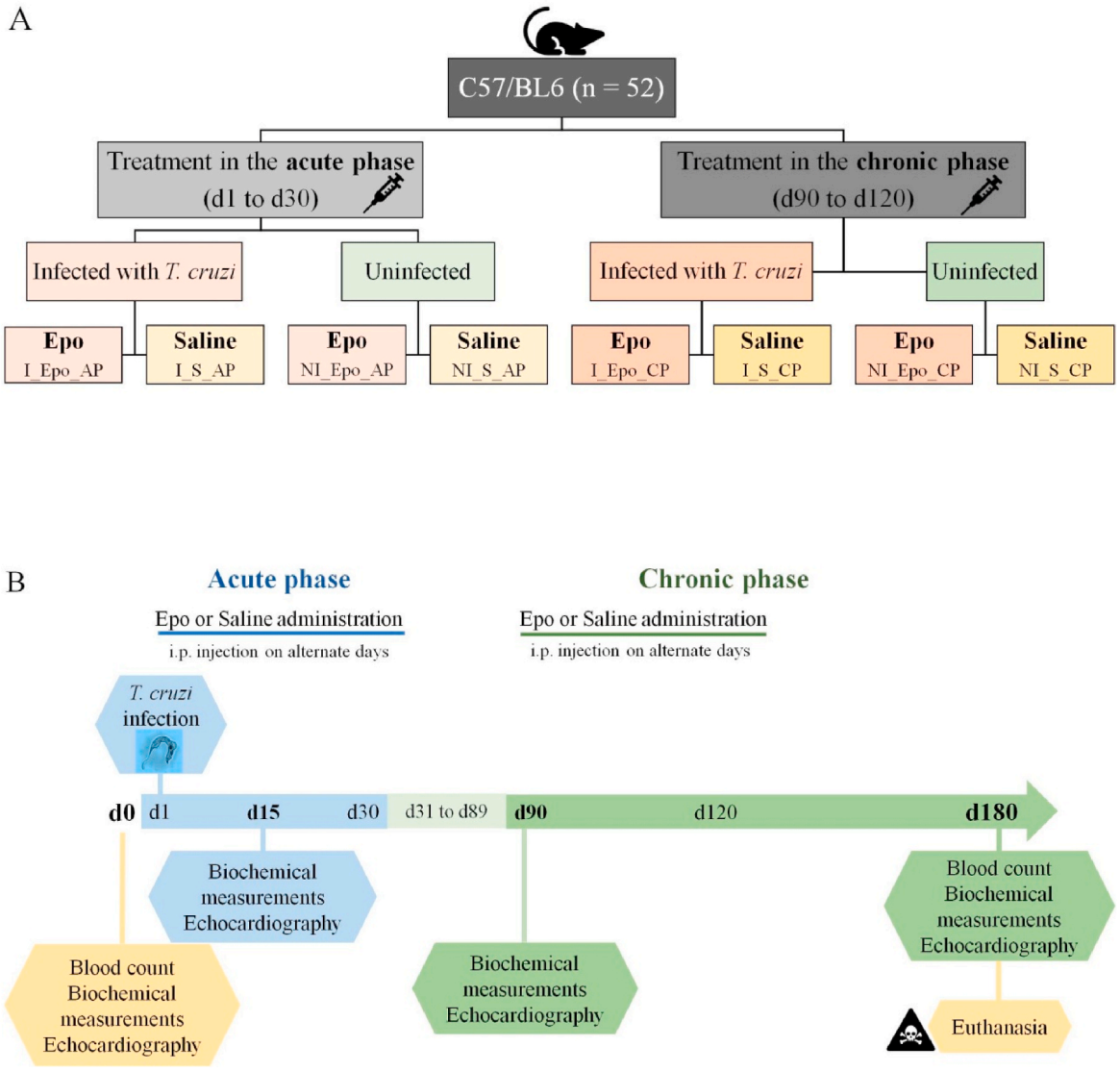

Fig. 1. Experimental design. **A.** Distribution of experimental groups. **B.** Experiment timeline. Epo: erythropoietin. I_Epo_AP: infected with *T. cruzi* and treated with Epo in the acute phase (d1 to d30). I_S_AP: infected and treated with saline in the acute phase. NI_Epo_AP: uninfected and treated with Epo between d1 and d30. NI_S_AP: uninfected and treated with saline between d1 and d30. I_Epo_CP: infected with *T. cruzi* and treated with Epo in the chronic phase (d90 to d120). I_S_CP: infected and treated with saline in the chronic phase. NI_Epo_CP: uninfected and treated with Epo between d90 and d120. NI_S_CP: uninfected and treated with saline between d90 and d120. d represents the experimental day (0–180). The acute and chronic phases represent the stage of Chagas disease.

2.5. Cellular damage markers

Blood from the orbital sinus was collected without anticoagulant and the serum was obtained by centrifugation. Then, serum was diluted in saline solution (1:3) to acquire the necessary volume for the assays. The activity of aspartate aminotransferase (AST), the total creatine kinase (CK), and the creatine kinase myocardial band (CK-MB) were used for assessing cardiac integrity. They were measured at d0, d15, d90, and d180 (i.e. twice in the acute phase and twice in chronic phase for infected groups) using specific commercial kits (Roche® Diagnostics) according to manufacturer recommendations. After the measurements, the results were multiplied by the dilution factor for correction. All biochemical dosages were performed on automated equipment (Cobas® C-111, Roche Diagnostics).

2.6. Functional analysis

Transthoracic echocardiography (Echo) was performed in all groups in d0, d15, d90, and d180 using the echo machine Vivid S6 (GE Healthcare®) with a sector ultrasound transducer to assess global left ventricular (LV) systolic function. Before collecting data, the animals were i.p. sedated with ketamine (50 μg/g) and xylazine (5 μg/g) (Stypmann et al., 2002). To avoid bias due to anesthesia the timing between induction and measurement was carefully controlled as recommended by Roth et al. and Rottman et al. (Roth et al., 2002; Rottman et al., 2003). The echocardiographic modalities evaluate were two-dimensional (2-D) brightness mode (B-mode) and motion mode (M-mode) according to the guidelines of the American Society of Echocardiography and the Guidelines for measuring cardiac physiology in mice (Lindsey et al., 2018). At least three data series were recorded for each animal. A single experienced veterinarian carried out all echocardiographs in a blind manner.

Through echocardiographic images obtained through the short axis, with the cursor directed equidistant of the LV papillary muscles in the chordal plane, the following variables were analyzed: LV end-diastolic diameter (LVEDD), LV end-systolic diameter (LVESD), LV posterior wall thickness in diastole (LVPWD), LV ejection fraction (EF), and fractional shortening (FS). EF and FS are calculated based on LV

chamber diameter and volume. The latter was calculated as [(LVEDD-LVESD)/LVEDD] x 100 (He et al., 2019).

The left ventricular systolic function was estimated through the EF and the fractional shortening (FS). Both provided as percentage values during systole compared with diastole. FS indicates the percentage change in LV chamber size and is an index of myocyte contraction, whereas EF indicates the percentage change in LV volumes and is an index of LV function. The level of cardiac impairment was assessed using the American Society of Echocardiography's Guidelines for humans using as a parameter the EF. The limit of normality for EF was defined as 55% (Lang et al., 2005). Values obtained by Vinhas et al. (2013) in adult mice were also used to analyze the results.

2.7. Tissue collection

After 180 days of infection or in an equivalent period for the non-infected animals, mice were anesthetized with 10% ketamine hydrochloride and 2% xylazine hydrochloride based on their body weight (2:1; maximal dose 10 mL/kg) (Syntec). Intracardiac blood samples were taken for hematologic examination, biochemical evaluation, serum recovery, and DNA extraction. After that, mice were euthanized with a lethal dose of anesthetics (ketamine/xylazine). The heart, spleen, and large intestine (colon) were removed. The heart and spleen were weighed and photographed. Part of the three tissues was placed in 4% formaldehyde for histopathological studies and the remainder was macerated separately and placed in 200 μL of lysis buffer (Mini Spin Plus Biopur; Biometrix) to obtain DNA.

2.8. Dosage of anti-T. cruzi antibodies

Serum from collected blood samples in d180 was separated by centrifugation. Detection of anti-*T. cruzi* immunoglobulin G (IgG) antibodies were assessed by Indirect Enzyme-linked Immunosorbent assay (ELISA) following protocols previously standardized in our laboratory (Hecht et al., 2010; Ribeiro et al., 2016). Every sample was run in triplicate. Cut-off values were determined using the optical density (OD) mean value plus three standard deviations of negative controls sera. Antibody levels, in arbitrary units (AU), were calculated as the ratio OD value of each serum sample/cut-off value (Longhi et al., 2012). Samples with OD 10% above the cut-off were considered positive. Likewise, samples with inferior OD compared to cut-off value were considered negative.

2.9. DNA extraction procedures and parasite load

To build a standard curve to quantify the *T. cruzi* by real-time PCR (qPCR), the parasite DNA was extracted from a culture of epimastigotes forms following a standard phenol-chloroform protocol (Wincker et al., 1994). Genomic DNA from mice tissue was obtained using the commercial kit Mini Spin Plus Biopur® (Biometrix) according to the manufacturer's instructions. For blood, it was used 200 μL of sample. For heart, spleen, and large intestine DNA, 20 mg of each tissue was macerated in lysis buffer and 200 μL was used for DNA isolation. The concentration of eluted DNA was measured by spectrophotometer (NanoVue® PlusSpectrophotometer, GE Healthcare) and the purity was determined at 260/280 nm. The extracted DNA was stored at −20 °C until its analysis.

To verify the DNA integrity and the absence of inhibitors, the constitutive β-actin gene was amplified by conventional PCR (cPCR). Amplified products were subjected to electrophoresis in 1% agarose gel containing 0.5 μg/mL of ethidium bromide and visualized under ultraviolet light.

Then, qPCR was performed for absolute quantification of *T. cruzi* nuclear DNA (nDNA) in blood, heart, spleen, and large intestine samples. A *T. cruzi* standard calibration curve was built with ten-fold serial dilutions of parasite DNA to cover a range between 10^{-3} to 10^{2} parasites to establish the DNA parasitic load in tissues of infected mice. The reaction mix consisted of 0.2 μM of each primer TCZ3 (5′ TGC ACT CGG CTG ATC GTT T 3′) and TCZ4 (5′-ATT CCT CCA AGC AGC GGA TA 3′), 10 μM of PowerUp SYBR® Green Master Mix (Applied Biosystems), 30 ng of template DNA in a final volume of 20 μL. The cycle condition was as follows: 50 °C for 2 min (to activate uracil-DNA glycosylase), 95 °C for 10 min, 40 cycles of 95 °C for 15 s, 60 °C for 45 s, and 72 °C for 10 s. A dissociation step (melting curve analysis) was made at the end of thermal cycling from 60 to 95 °C. The specificity of the amplified products was checked by analysis of the melting curve.

In each run, two negative controls (samples without DNA and mouse samples known negative for *T. cruzi*) were included. To avoid differences in multi-plate measurements, two *T. cruzi* total DNA samples (10^{-1} and 10^{2} parasites) were also added to each plate and used as calibrators, applying a between-run correction factor, according to Ruijter et al. (2015). Each sample was analyzed in duplicate. The duplicate values were averaged, and parasite load was calculated by plotting the quantification cycle values (Cq) against each standard of known concentration and calculation of the linear regression line of the standard curve and expressed as parasites equivalent/30 ng of total DNA. All the assays were performed in 96-well plates (Optical 96-Well Reaction Plate, MicroAmp®) using StepOne® Plus Real-Time PCR Systems (Applied Biosystems, CA, USA).

2.10. Histopathological analysis

Samples of heart, spleen, and large intestine from all animals were fixed in 10% buffered formaldehyde and then were dehydrated through a series of ascending ethanol concentrations, diaphanized with xylene, and paraffin embedded. Three serial sections at 5 μm thicknesses of different parts of each tissue were cut with a microtome and stained with hematoxylin and eosin (H&E) for histopathological analysis in a blind manner under an optical microscope (Olympus BX51 U-LH100HG, Olympus). The ScanScope (Aperio®) was employed to record the images.

The evaluation of tissue response was based on qualitative and quantitative analysis of infected and uninfected *T. cruzi* tissues, treated or not with Epo. For this, cardiomyocyte necrosis, multifocal perivascular mononuclear infiltrate, multifocal interstitial mononuclear infiltrate, and cardiac fibrosis (interstitial collagen deposition); spleen follicular hyperplasia and multifocal mononuclear inflammatory infiltrate in the intestine were quantitatively scored into: 0 (absent); 1 (mild - 2 to 15% of the entire section); 2 (moderate - 16 to 60% of the entire section) and 3 (severe - over 60% of the section). The presence or absence of amastigote nests in cardiac tissue was also evaluated, with the following classification: 0 (absent); 1 (rare - an amastigote nest observed in two sections); 2 (moderate - 2 to 10 nests); and 3 abundant (more than 10 nests) (modified from Castro-Sesquen et al., 2011). Numerical values of each parameter of each animal for the different experimental groups were used for statistical analysis.

Fig. 1B illustrates the timeline of the experiments.

2.11. Statistical analysis

The experiment followed a factorial design [2 infection *status* (infected and not infected) x 2 substances (Epo and Saline) x 2 periods of substance administration (acute and chronic)]. For these 8 combinations (2 infection *status* x 2 substances x 2 periods of substance administration) there were at least five mice as replicates. All statistical analyses were performed using SAS® (v9.4, Cary, North Carolina) with 5% of significance level.

Collected data were subjected to analysis of normality using the Shapiro-Wilk test. Data from echocardiography, hematology, and biochemical variables were submitted to a repeated measures analysis using PROC MIXED with compound symmetry (CS) as covariance structure. Tukey test was used to compare means. Non-parametric data

were analyzed using PROC GLIMMIX using infection, substance, and experimental day as independent variables. For histopathological data, the experimental day was excluded from analysis. Finally, quantitative data was submitted to a correlation analysis using PROC CORR.

3. Results

3.1. Effect of erythropoietin on hematological parameters

Hematocrit (Hct) was similar in all experimental groups before saline or Epo administration. As expected, Epo treatment induced erythrocytosis. The Hct was on average 41% higher in Epo-treated groups at the end of treatment (30 days of administration).

Table 1 shows all the values of the red blood cell parameters measured at d0 and d180. At d180, Hct remained high in Epo-treated groups (46.84 ± 2.46%) compared to saline groups (40.62 ± 6.07%) (effect of substance, $p < 0.0001$). An effect of substance ($p = 0.022$) was also found in HGB with Epo-treated animals with higher values than untreated mice (12.75 ± 0,26 g/100 mL and 11.59 ± 0.33 g/100 mL, respectively). Regarding the RBC at d180, infected groups showed higher values than non-infected ones ($8.56 \pm 0.95 \times 10^6/mm^3$ and $7.49 \pm 1.18 \times 10^6/mm^3$, respectively; effect of infection, $p = 0.014$).

When the hematological parameters measured in d0 and d180 were compared within the same group, only in animals from NI_Epo_AP no difference was seen. The circulating levels of RBC declined significantly at d180 compared to d0 in NI_S_AP and I_Epo_AP ($p = 0.010$ and 0.006, respectively). An increase at HGB at the end of the experimental period was observed in NI_Epo_CP ($p = 0.009$) and I_S_CP ($p = 0.025$) groups, while it declined in NI_S_AP ($p = 0.004$), I_S_AP ($p = 0.025$), and I_Epo_AP ($p = 0.002$) (Table 1).

Concerning the white series, neither basophils nor immature neutrophils were found in any mouse. At d0 mice that received saline in the acute phase (infected and not infected by *T. cruzi*) had higher values of WBC (substance x period interaction, $p < 0.0001$). The same was observed in the absolute values of lymphocytes ($p < 0.0001$) and monocytes ($p = 0.022$). At d180 an interaction between infection x substance x period of substance administration was observed in WBC ($p = 0.044$) and lymphocytes ($p = 0.011$). Infected animals, regardless of treatment with Epo, showed higher values of WBC compared to the following groups of uninfected animals: NI_S_AP, NI_S_CP, and NI_Epo_CP (Table 2). On lymphocytes, infected mice that received saline had lower values than infected animals treated with Epo (Table 2). An effect of infection was observed in monocytes ($p < 0.0001$) and segmented neutrophils ($p = 0.021$). In both variables, infected mice showed higher values than uninfected animals. Table 2 shows the values of the white-blood series measured at d0 or d180.

The comparison within the same group of white cells parameters showed a significant decrease from d0 to d180 in WBC counts in NI_S_AP ($p = 0.003$), NI_S_CP ($p = 0.041$), NI_Epo_CP ($p = 0.006$), and I_S_AP ($p = 0.018$), whereas an increase was observed in I_S_CP ($p = 0.049$). No difference was observed between d0 and d180 in the other groups. Lymphocytes were lower at d180 comparing to d0 in three non-infected groups: NI_S_AP ($p = 0.004$), NI_S_CP ($p = 0.041$), NI_Epo_CP ($p = 0.006$). In the other groups, no changes were noted (Table 2). Absolute monocytes raised at d180 for the groups I_Epo_AP ($p = 0.004$) and I_S_CP ($p = 0.049$). Segmented neutrophils decreased at d180 in NI_S_AP group ($p = 0.004$), while in the NI_Epo_CP group, a decline was observed in eosinophils ($p = 0.0360$) (Table 2).

3.2. Effect of erythropoietin on biochemical parameters

AST concentration was similar among all groups at the beginning of the experiment (d0). In the infected groups, Epo-treated or not, the AST concentration had increased through the infection course with the level at d0 significantly lower from d15, d90, and d180 (interaction between infection x day experimental; $p < 0.0001$). Conversely, uninfected Epo-treated or untreated mice showed similar levels at d0, d15, and 180 (Supplementary Table 1).

Considering each group throughout the experimental period, it was possible to verify that in absence of *T. cruzi* infection, serum AST levels remained the same over time regardless of Epo treatment. The exception was the group NI_S_CP in which the values at d15 were lower than those measured in any other period ($p = 0.018$), whereas at d90 and d180 they were similar to the initial time point (Table 3). With the infection and in the absence of Epo treatment (I_S_AP and I_S_CP), the activity of AST increased after d0 ($p < 0.05$), remaining the same at d15, d90, and d180. The combination of *T. cruzi* infection and Epo-treatment showed lower levels of AST in d0 compared to later periods ($p < 0.006$). Actually, in the group I_Epo_AP the following order was observed: d0 < d15 > d90 = d180 ($p < 0.03$), whereas in I_Epo_CP we identified that d0 < d15 = d180 > d90 (Table 3).

An effect of experimental day ($p = 0.0101$) was found in serum activity of CK showing that the total average of all groups was lower at d0 than d90 (340.09 ± 413.28 U/L and 592.20 ± 597.36 U/L, respectively). In NI_Epo_CP group no change in serum CK was observed in d180 compared to d0. Conversely, in NI_Epo_AP group the CK levels were higher in d180 versus d0. The analysis of the measured values in each group showed no significant difference in NI_S_AP, NI_S_CP, I_S_CP, and I_Epo_CP.

At d180 uninfected Epo-treated mice had lower CK-MB values than uninfected untreated animals at the same time (223.63 ± 53.04 U/L and 539.58 ± 116.16 U/L, respectively; interaction infection x substance x experimental day, $p = 0.0002$). Actually, in mice treated with Epo lower levels of CK-MB were found compared to those who received saline (effect of substance, $p = 0.01$), whereas an effect of infection alone was not observed.

Table 1
Red blood cell parameters at the beginning and end of the experimental period.

		NI_S_AP	NI_Epo_AP	I_S_AP	I_Epo_AP	NI_S_CP	NI_Epo_CP	I_S_CP	I_Epo_CP
RBC (x10^6/mm^3)	**d0**	10.62 ± 1.96^{Aa}	6.80 ± 1.36^{Aa}	9.14 ± 0.31^{Aa}	9.45 ± 0.49^{Aa}	9.48 ± 1.86^{Aa}	8.56 ± 1.93^{Aa}	7.84 ± 1.22^{Aa}	8.92 ± 0.84^{Aa}
	d180	7.11 ± 1.58^{Ba}	7.72 ± 0.78^{Aa}	8.61 ± 0.54^{Aa}	8.53 ± 0.66^{Ba}	7.76 ± 0.93^{Aa}	7.44 ± 1.34^{Aa}	7.21 ± 1.05^{Aa}	9.34 ± 0.84^{Ab}
Hct (%)	**d0**	45.67 ± 2.88^{Aa}	45.75 ± 2.87^{Aa}	45.40 ± 3.21^{Aa}	49.14 ± 1.77^{Aa}	47.43 ± 3.46^{Aa}	47.80 ± 0.45^{a}	47.67 ± 1.86^{Aa}	46.71 ± 1.89^{Aa}
	d180	35.50 ± 4.51^{Ba}	48.20 ± 2.77^{Aa}	39.80 ± 6.06^{Aa}	47.00 ± 3.06^{Aa}	44.50 ± 5.35^{Aa}	Not available	42.50 ± 0.71^{Aa}	45.71 ± 0.76^{Aa}
HGB (g/100 mL)	**d0**	18.65 ± 3.42^{Aa}	9.73 ± 0.67^{Aa}	15.60 ± 0.72^{Aa}	15.74 ± 0.40^{Aa}	14.87 ± 3.05^{Aa}	9.26 ± 0.68^{Aa}	9.08 ± 1.10^{Aa}	14.13 ± 1.33^{Aa}
	d180	11.65 ± 1.48^{Ba}	12.85 ± 0.64^{Aa}	11.22 ± 1.66^{Ba}	12.39 ± 1.03^{Ba}	11.48 ± 1.53^{Aa}	13.00 ± 0.47^{Ba}	12.00 ± 1.44^{Ba}	12.76 ± 1.97^{Aa}

Values are means ± standard deviation.
Different uppercase letters in the same column within the variable are significantly different ($p \leq 0.05$).
Different lower-case letters in the same row are significantly different ($p \leq 0.05$).
RBC: Red blood cell count. Hct: Hematocrit. HGB: Hemoglobin. d0: the beginning of the study. d180: end of the trial. NI_S_AP: uninfected and treated with saline between d1 and d30. NI_Epo_AP: uninfected and treated with erythropoietin (Epo) between d1 and d30. I_S_AP: infected with *T. cruzi* and treated with saline in the acute phase (d1 to d30). I_Epo_AP: infected and treated with Epo in the acute phase. NI_S_CP: uninfected and treated with saline between d90 and d120. NI_Epo_CP: uninfected and treated with Epo between d90 and d120. I_S_CP: infected with *T. cruzi* and treated with saline in the chronic phase (d90 to d120). I_Epo_CP: infected and treated with Epo in the chronic phase.

Table 2
Evaluation of the white blood cells with differential absolute leukocyte count at the beginning and end of the experimental period.

		NI_S_AP	NI_Epo_AP	I_S_AP	I_Epo_AP	NI_S_CP	NI_Epo_CP	I_S_CP	I_Epo_CP
WBC ($x10^3/mm^3$)	**d0**	10.50 ± 1.84^{A}	4.95 ± 1.21^{A}	11.90 ± 2.10^{A}	6.54 ± 1.53^{A}	4.30 ± 1.14	4.34 ± 1.09^{A}	3.76 ± 0.44^{A}	5.09 ± 2.61^{A}
	d180	2.08 ± 0.81^{Ba}	5.75 ± 1.20^{Aab}	6.02 ± 1.60^{Bb}	6.24 ± 1.96^{Ab}	2.69 ± 1.14^{a}	2.66 ± 0.47^{Ba}	6.87 ± 3.07^{Bb}	7.52 ± 0.68^{Ab}
Lymphocytes ($x10^3/mm^3$)	**d0**	8.81 ± 1.30^{A}	4.04 ± 1.03^{A}	9.75 ± 1.58^{A}	5.65 ± 1.38^{A}	3.62 ± 1.06^{A}	3.70 ± 0.93^{A}	2.87 ± 0.30^{A}	4.09 ± 2.08^{A}
	d180	1.64 ± 0.73^{Ba}	4.99 ± 1.16^{Abc}	3.87 ± 1.98^{Bab}	5.12 ± 1.79^{Ac}	2.05 ± 0.94^{Bab}	1.97 ± 0.48^{Bab}	2.76$^{\#Aab}$	6.03 ± 0.84^{Ac}
Monocytes ($x10^3/mm^3$)	**d0**	0.32 ± 0.16^{A}	0.13 ± 0.06^{A}	0.41 ± 0.43^{A}	0.19 ± 0.13^{A}	0.10 ± 0.09^{A}	0.15 ± 0.12^{A}	0.12 ± 0.06^{A}	0.13 ± 0.07^{A}
	d180	0.24 ± 0.24^{A}	0.16 ± 0.15^{A}	0.84 ± 0.11^{A}	0.51 ± 0.15^{B}	0.26 ± 0.32^{A}	0.15 ± 0.48^{A}	0.24$^{\#A}$	0.54 ± 0.22^{B}
Segmented neutrophils ($x10^3/mm^3$)	**d0**	1.33 ± 0.67^{Abc}	0.74 ± 0.23^{Aab}	2.19 ± 0.74^{Ac}	0.63 ± 0.33^{Aab}	0.55 ± 0.07^{Aab}	0.46 ± 0.09^{Aa}	0.63 ± 0.20^{Aab}	0.82 ± 0.57^{Aab}
	d180	0.24 ± 0.11^{B}	0.61 ± 0.11^{A}	1.14 ± 0.96^{A}	0.55 ± 0.10^{A}	0.35 ± 0.20^{A}	0.54 ± 0.24^{A}	0.60$^{\#A}$	0.90 ± 0.35^{A}
Eosinophils ($x10^3/mm^3$)	**d0**	0.04 ± 0.06^{A}	0.04 ± 0.04^{A}	0.00 ± 0.00^{A}	0.07 ± 0.07^{A}	0.03 ± 0.03^{A}	0.03 ± 0.02^{A}	0.01 ± 0.02^{A}	0.02 ± 0.04^{A}
	d180	0.03 ± 0.03^{A}	0.00 ± 0.00^{A}	0.54 ± 0.99^{A}	0.06 ± 0.06^{A}	0.03 ± 0.03^{A}	0.00 ± 0.00^{B}	0.00 ± 0.00^{A}	0.05 ± 0.04^{A}

Values are means ± standard deviation.
Different uppercase letters in the same column within the variable are significantly different ($p \leq 0.05$).
Different lower-case letters in the same row are significantly different ($p \leq 0.05$).
#Value of just one mouse.
WBC: white blood cells. d0: the beginning of the study. d180: end of the trial. NI_S_AP: uninfected and treated with saline between d1 and d30. NI_Epo_AP: uninfected and treated with erythropoietin (Epo) between d1 and d30. I_S_AP: infected with *T. cruzi* and treated with saline in the acute phase (d1 to d30). I_Epo_AP: infected and treated with Epo in the acute phase. NI_S_CP: uninfected and treated with saline between d90 and d120. NI_Epo_CP: uninfected and treated with Epo between d90 and d120. I_S_CP: infected with *T. cruzi* and treated with saline in the chronic phase (d90 to d120). I_Epo_CP: infected and treated with Epo in the chronic phase.

Table 3
Serum biochemical parameters measured in each group throughout the study period.

Groups	AST (U/L)				CK (U/L)				CK-MB (U/L)			
	d0	d15	d90	d180	d0	d15	d90	d180	d0	d15	d90	d180
NI_S_AP	98.25 ± 54.52	90.86 ± 28.45	171.86 ± 159.89	109.20 ± 29.36	771.27 ± 836.11	302.90 ± 205.02	619.75 ± 463.06	795.12 ± 566.73	525.48 ± 208.80	439.14 ± 175.42	530.96 ± 188.02	486.22 ± 115.98
NI_Epo_AP	72.0 ± 21.0	85.80 ± 31.51	117.60 ± 68.85	100.20 ± 17.18	220.0 ± 176.06a	292.08 ± 322.15 ab	802.44 ± 802.02b	615.36 ± 124.92b	402.00	293.16 ± 63.82	376.05 ± 163.74	232.62 ± 51.22
I_S_AP	106.5 ± 35.45a	184.20 ± 66.53b	215.25 ± 64.50b	186.0 ± 56.88b	334.58 ± 210.66 ab	315.36 ± 175.19a	1053.53 ± 749.68b	544.74 ± 454.28 ab	421.73 ± 236.08	320.40 ± 65.52	687.53 ± 216.22	373.65 ± 151.22
I_Epo_AP	74.50 ± 22.64a	251.14 ± 64.43c	152.14 ± 41.77b	180.0 ± 60.97b	159.90 ± 102.63a	663.75 ± 312.88c	292.60 ± 129.65 ab	366.30 ± 187.56b	245.94 ± 72.13a	413.40 ± 96.16bc	350.23 ± 90.08 ab	531.00 ± 123.66c
NI_S_CP	113.63 ± 24.97b	74.14 ± 22.89a	162.86 ± 97.81b	102.75 ± 9.60b	253.75 ± 117.06	190.54 ± 80.91	710.96 ± 818.24	282.90 ± 82.74	382.44 ± 119.41a	269.70 ± 152.99a	378.25 ± 131.93a	628.50 ± 36.73b
NI_Epo_CP	95.25 ± 38.45	73.20 ± 18.07	121.8 ± 96.50	144.60 ± 95.92	690.48 ± 904.58b	170.28 ± 77.51a	732.30 ± 922.05b	892.62 ± 746.68b	481.05 ± 67.00b	277.38 ± 107.59a	341.70 ± 250.15 ab	214.64 ± 59.20a
I_S_CP	87.0 ± 16.43a	234.60 ± 94.90b	159.75 ± 38.76b	171.6 ± 68.78b	228.15 ± 115.83	592.50 ± 606.49	380.48 ± 198.93	252.54 ± 87.68	439.40 ± 299.08	339.23 ± 115.22	358.10 ± 202.01	198.50 ± 106.88
I_Epo_CP	90.43 ± 14.43a	200.57 ± 33.52c	131.63 ± 21.24b	190.13 ± 41.47c	276.73 ± 98.55	240.26 ± 92.39	348.56 ± 200.93	293.13 ± 193.74	455.49 ± 133.58b	429.75 ± 59.28 ab	302.40 ± 81.19a	287.69 ± 152.21a

Values are means ± standard deviation.
Different lower-case letters in the same row within the same variable are significantly different ($p \leq 0.05$).
AST: aspartate aminotransferase. CK: the total creatine kinase. CK-MB: creatine kinase myocardial band. d: day experimental (0–180). NI_S_AP: uninfected and treated with saline between d1 and d30. NI_Epo_AP: uninfected and treated with erythropoietin (Epo) between d1 and d30. I_S_AP: infected with *T. cruzi* and treated with saline in the acute phase (d1 to d30). I_Epo_AP: infected and treated with Epo in the acute phase. NI_S_CP: uninfected and treated with saline between d90 and d120. NI_Epo_CP: uninfected and treated with Epo between d90 and d120. I_S_CP: infected with *T. cruzi* and treated with saline in the chronic phase (d90 to d120). I_Epo_CP: infected and treated with Epo in the chronic phase.

There was no difference in this variable over time in NI_S_AP, NI_Epo_AP, I_S_AP, and I_S_CP. Despite the absence of infection, in the group NI_S_CP, the measured values at d180 were significantly greater than the other periods ($p < 0.04$). The serum activity of CK-MB was higher at d180 than d0 in mice from I_Epo_AP group ($p < 0.04$). In contrast, chronic Epo administration reduced CK-MB serum activity from d0 to d180 irrespectively of *T. cruzi* infection ($p < 0.04$).

3.3. Anti-Trypanosoma cruzi antibodies production

After 180 days of *T. cruzi* infection, all mice produced anti-*T. cruzi* IgG antibodies at similar levels, regardless of Epo treatment (Supplementary Table 2).

3.4. Echocardiographic parameters

In the baseline (d0) there was no difference in EF nor in FS between groups. At d90 infected mice Epo-treated showed EF lower than infected

mice untreated (saline only) (59.60 ± 16.86% vs 77.78 ± 11.56%; interaction infection x substance at d90, p = 0.002) indicating a negative effect of Epo at this time point. The same was observed in FS (28.13 ± 10.26% vs 42.11 ± 11.16%; interaction infection x substance at d90, p = 0.0006). However, at d180 no difference was observed in FS. In this same time point, a significant interaction between infection, substance, and period of substance administration was observed in EF (p = 0.038) showing that I_Epo_AP group was different from I_Epo_CP (44.71 ± 17.89% vs 72.13 ± 7.34%) (Supplementary Fig. 1).

Analyzing individually each group, EF and FS were preserved throughout the experimental period, except for the group I_Epo_AP. In this one, the EF and FS were maintained during the treatment with Epo (d0 to d15), however, after 180 days of infection, a significant reduction in both parameters could be observed compared to d15 (for EF 77.0 ± 15.92% vs 44.71 ± 17.89%, p = 0.03 and for FS 42.57 ± 15.18% vs 19.57 ± 8.96%, p = 0.023 at d15 and d180). Of note, in this group, the EF value at d180 was lower than that considered normal for humans (≥55%) and out the reference value established by Vinhas et al. (2013) (Vinhas et al., 2013) (Supplementary Fig. 1).

Fig. 2 classifies the mice at d180 according to the degree of cardiac impairment as a function of EF according to the American Society of Echocardiography's Guidelines (i.e. frequency of mice in each group showing cardiac alteration). As mentioned before, at d180 the only significant difference observed was between I_Epo_AP and I_Epo_CP. In the last group, 100% of mice had normal EF. In contrast, in the I_Epo_AP group, only 28.57% (2/7 mice) had normal EF, the same amount had mild systolic dysfunction, 14.29% (1/7) was moderately abnormal, and 28.57% (2/7) presented severe cardiac impairment. It is important to point out that in this group, at d180 the mean value of EF was 44.71 ± 17.89%, a value below what is considered normal for mice (for review, see Stypmann et al., 2009) and determinate by Vinhas et al. (2013) (Fig. 2). Sixty percent of infected animals who received saline (acute or chronic phase) had no systolic dysfunction (EF ≥ 55%). This number was slightly higher in infected Epo-treated mice, in which the absence of cardiac impairment was shown in 66.67% of animals.

It was observed that after 15 days of Epo treatment, the LVPWD in infected mice was significantly different from infected without Epo (1.04 ± 0.39 mm for I_Epo_AP and 1.17 ± 0.39 mm for I_S_AP; interaction infection x substance x period of treatment, p = 0.023). At d90 an interaction substance x period was seen in mice that received Epo or saline in the acute phase. Once again, Epo-treated presented lower values of LVPWD (1.04 ± 0.39 mm for Epo_AP and 1.16 ± 0.37 mm for S_AP, p = 0.013). On the other hand, at d180 only an effect of infection was found (1.05 ± 0.22 mm for uninfected mice and 1.10 ± 0.30 mm for infected ones; p = 0.049). The analysis of each group separately showed no ventricular hypertrophy, evaluated by LVPWD.

3.5. Parasitic load

The qPCR performed at d180 allowed the detection of *T. cruzi* DNA in all infected samples of blood, heart, and large intestine. In only one spleen mouse DNA of I_Epo_AP group, the parasitemia was not detected, just as it was absent in all tissues of uninfected animals. In fact, the spleen parasitism was particularly low with five samples with quantification at the detection limit of our methods. In all groups, except for I_S_AP, the mean of parasitic load in the spleen was lower than the other tissues within the same group (Fig. 3).

The number of parasites varied between animals belonging to the same group. As expected, Epo did not present a trypanocide effect. The blood parasitemia tended to be higher in Epo treated mice (I_Epo_AP and I_Epo_CP) compared to saline ones (I_S_AP and I_S_CP). In the heart, parasite DNA amount was much less than blood in Epo-treated groups (I_Epo_AP and I_Epo_CP; p < 0.0001), conversely to Epo untreated-infected groups in which similar parasitism was observed in both tissues. Of note, the large intestine was the only tissue that the parasite number was comparable among infected groups regardless of the Epo treatment (Fig. 3).

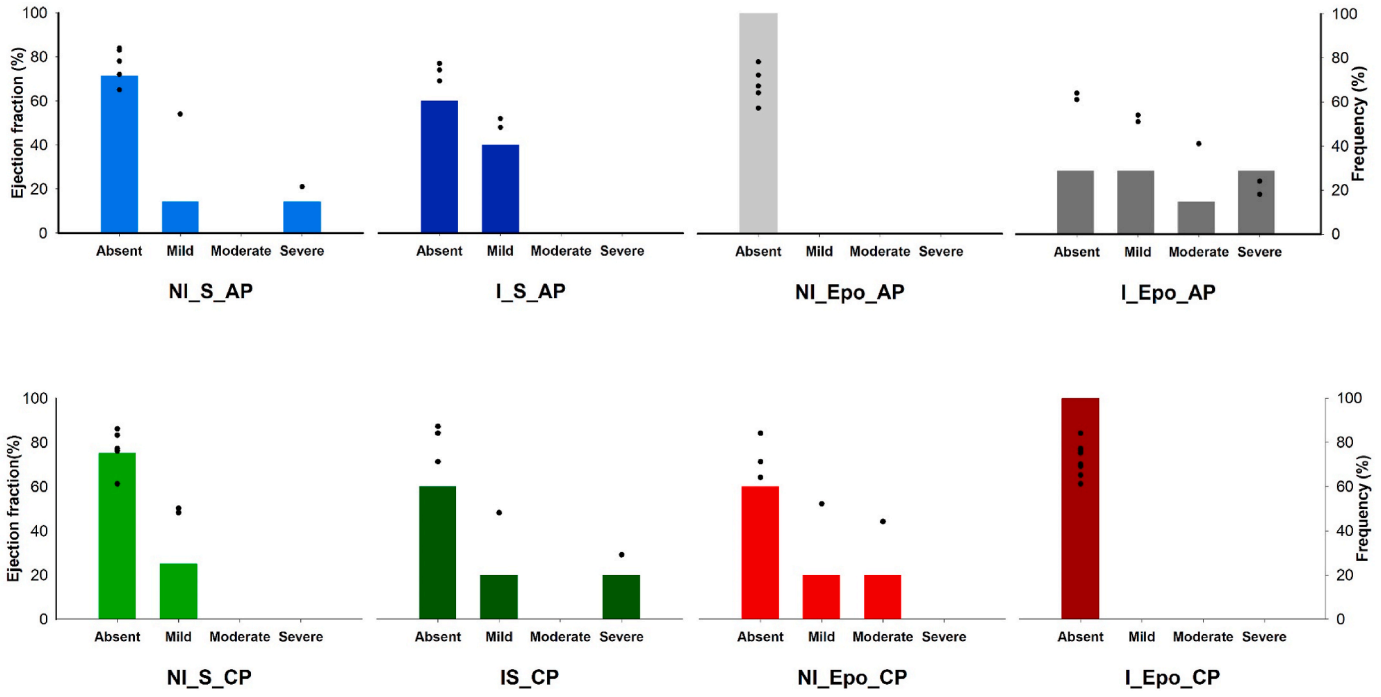

Fig. 2. Degree of cardiac involvement at the end of the experimental period (d180) using the left ventricular ejection fraction (EF) as a parameter. The left Y-axis indicates the EF. Each mouse is represented by a black circle. The right Y-axis represents the frequency of mice in each category of cardiac impairment. According to the American Society of Echocardiography's Guidelines EF ≥ 55% indicates absence of impairment, EF 45–54% is mildly abnormal, EF 30–44% is moderately abnormal, and EF <30% means a heart severely abnormal.

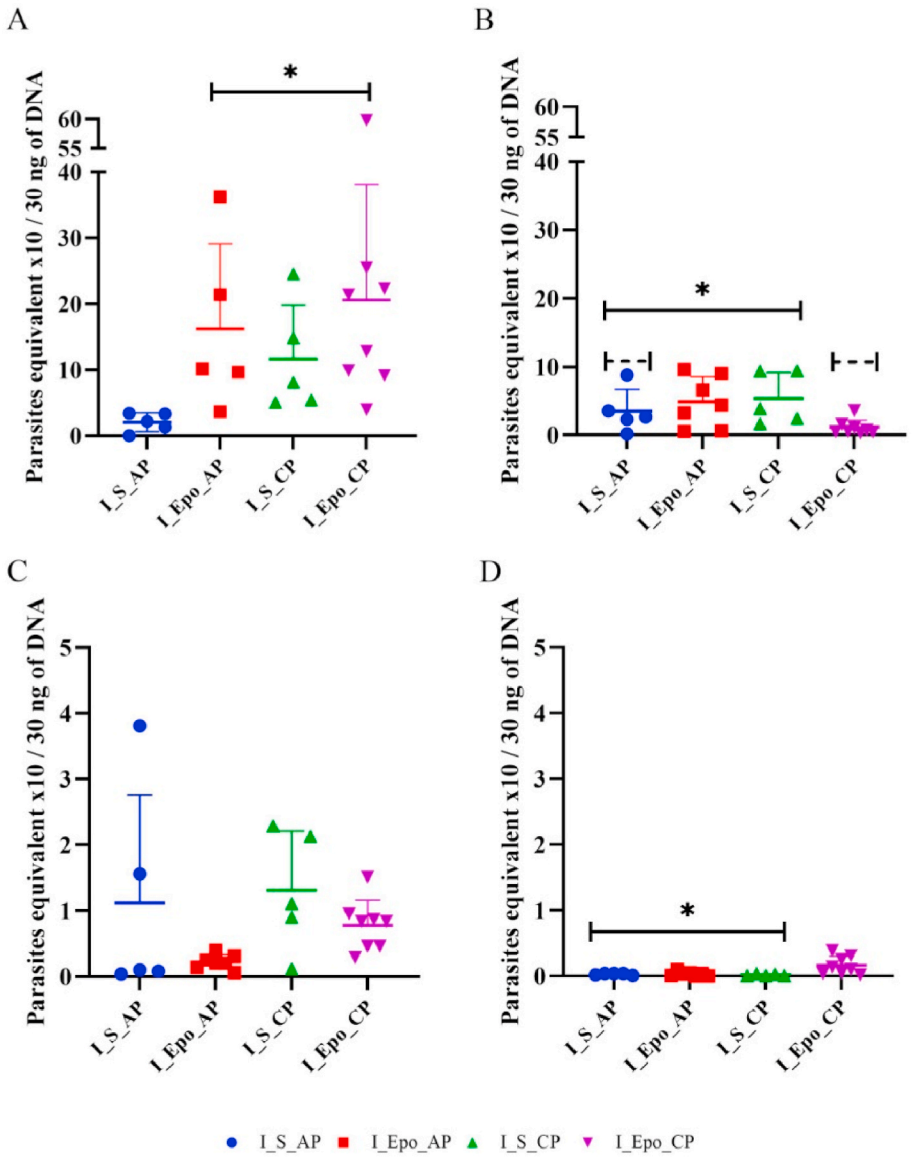

Fig. 3. Parasite burden of *Trypanosoma cruzi* infected groups. Blood (A), heart (B), large intestine (C), and spleen (D) samples were obtained after 180 days post-infection. DNAs were used as template in qPCR reactions using specific primers for *T. cruzi* nuclear DNA. Data points represent individual mice. Symbols indicate absolute levels and colored bars indicate mean and standard deviation. * Indicate that the parasite quantification is similar between groups under bars and significantly different from the other groups. $p < 0.05$. In B, the parasite quantification of groups under the dotted bars is not significantly different. No statistical difference was found in intestine (C).

3.6. Histopathologic analysis

During euthanasia, splenomegaly was seen in all infected animals (Epo-treated or not) with a significant difference in the spleen weight of these mice compared with uninfected ones ($p < 0.001$) (Table S3). Microscopically, it was found that infected animals presented spleen follicular hyperplasia more pronounced than uninfected mice ($p = 0.044$). Also, mice treated with Epo showed an average twice as many splenic changes ($p = 0.002$) compared to untreated mice (0.80 ± 0.60 vs 0.40 ± 0.58 arbitrary units, respectively) (Supplementary Fig. 2).

Uninfected animals, treated and untreated, exhibited no pathologic changes in the heart by light microscopy. Gross examination of the heart did not reveal cardiomegaly in any mice. In this sense, when the heart was weighed, no difference was shown between groups. The quantitative assessment revealed a cardioprotective effect of Epo in infected mice in relation to tissue necrosis ($p = 0.05$). In fact, cardiac necrosis was observed in 50% of infected untreated animals and only in 13% of infected Epo-treated mice (Table 4).

Cardiac fibrosis was observed only in acutely infected mice (treated or untreated) (14% of mice in I_Epo_AP group and 40% of I_S_AP; interaction between infection and phase, $p = 0.044$), while no chronic infected mice treated or not (I_Epo_CP and I_S_CP) presented fibrosis (Table 4). Multifocal inflammatory infiltrates in the perivascular and interstitial regions in the heart were present in all infected groups. No effect of Epo was observed (effect of infection only in both parameters, $p < 0.0001$). The quantitative assessment showed no difference between infected groups, even though only 37.5% of the animals in the I_Epo_CP group presented inflammation in the perivascular region whereas the rate in the other groups was more than 70% of mice (Table 4) (Fig. 4). Amastigote nests at d180 were found in the heart of only one mouse of the I_S_AP group.

The large intestine from any group of uninfected mice showed normal morphological appearance. *T. cruzi* infection had a significant effect on this tissue ($p < 0.0001$) causing multifocal mononuclear inflammatory infiltrate. An overall reduction was observed in the inflammatory process in groups treated with Epo (70% of infected untreated mice presented inflammation in the intestine, whereas this occurred in 53% of infected Epo-treated) (Table 4). Supplementary Fig. 3 shows representative images of histological findings in the intestine.

3.7. Correlation analysis

The interaction among antibody production against parasite

Table 4
Histopathology summary of tissue evaluation.

Experimental groups		Heart				Spleen	Large intestine
		Necrosis	Fibrosis	Inflammatory infiltrates (perivascular region)	Inflammatory infiltrates (interstitial region)	Follicular hyperplasia	Inflammatory infiltrates
NI_S_AP	Presence	0% (0/7)	0% (0/7)	0% (0/7)	0% (0/7)	28.6% (2/7)	0% (0/7)
	Quantification*	0	0	0	0	0.286 ± 0.488	0
NI_Epo_AP	Presence	0% (0/5)	0% (0/5)	0% (0/5)	0% (0/5)	80% (4/5)	0% (0/5)
	Quantification*	0	0	0	0	1.200 ± 0.837	0
I_S_AP	Presence	60% (3/5)	40% (2/5)	80% (4/5)	60% (3/5)	40% (2/5)	40% (2/5)
	Quantification*	0.600 ± 0.548	0.400 ± 0.548	0.800 ± 0.447	1.200 ± 1.095	0.400 ± 0.548	0.800 ± 1.095
I_Epo_AP	Presence	28.6% (2/7)	14.3% (1/7)	71.4% (5/7)	85.7% (6/7)	57.1% (4/7)	42.8% (3/7)
	Quantification*	0.286 ± 0.488	0.143 ± 0.378	0.714 ± 0.488	1.143 ± 0.690	0.571 ± 0.535	0.429 ± 0.535
NI_S_CP	Presence	0% (0/7)	0% (0/7)	0% (0/7)	0% (0/7)	57.1% (4/7)	0% (0/7)
	Quantification*	0	0	0	0	0.625 ± 0.744	0
NI_Epo_CP	Presence	0% (0/5)	0% (0/5)	0% (0/5)	0% (0/5)	100% (5/5)	0% (0/5)
	Quantification*	0	0	0	0	1.200 ± 0.447	0
I_S_CP	Presence	40% (2/5)	0% (0/5)	80% (4/5)	100% (5/5)	20% (1/5)	80% (4/5)
	Quantification*	0.400 ± 0.548	0	0.800 ± 0.447	1.400 ± 0.548	0.200 ± 0.447	1.000 ± 0.707
I_Epo_CP	Presence	0% (0/8)	0% (0/8)	37.5% (3/8)	87.5% (7/8)	75% (6/8)	62.5% (5/8)
	Quantification*	0	0	0.375 ± 0.518	1.000 ± 0.535	0.750 ± 0.463	0.625 ± 0.518

Presence: percentage of animals showing the characteristic. In brackets is the number of mice showing the characteristic/n in the group.
*total of quantified changes/n. Arbitrary units. Data expressed in average ± standard deviation. NI_S_AP: uninfected and treated with saline between d1 and d30. NI_Epo_AP: uninfected and treated with erythropoietin (Epo) between d1 and d30. I_S_AP: infected with *T. cruzi* and treated with saline in the acute phase (d1 to d30). I_Epo_AP: infected and treated with Epo in the acute phase. NI_S_CP: uninfected and treated with saline between d90 and d120. NI_Epo_CP: uninfected and treated with Epo between d90 and d120. I_S_CP: infected with *T. cruzi* and treated with saline in the chronic phase (d90 to d120). I_Epo_CP: infected and treated with Epo in the chronic phase.

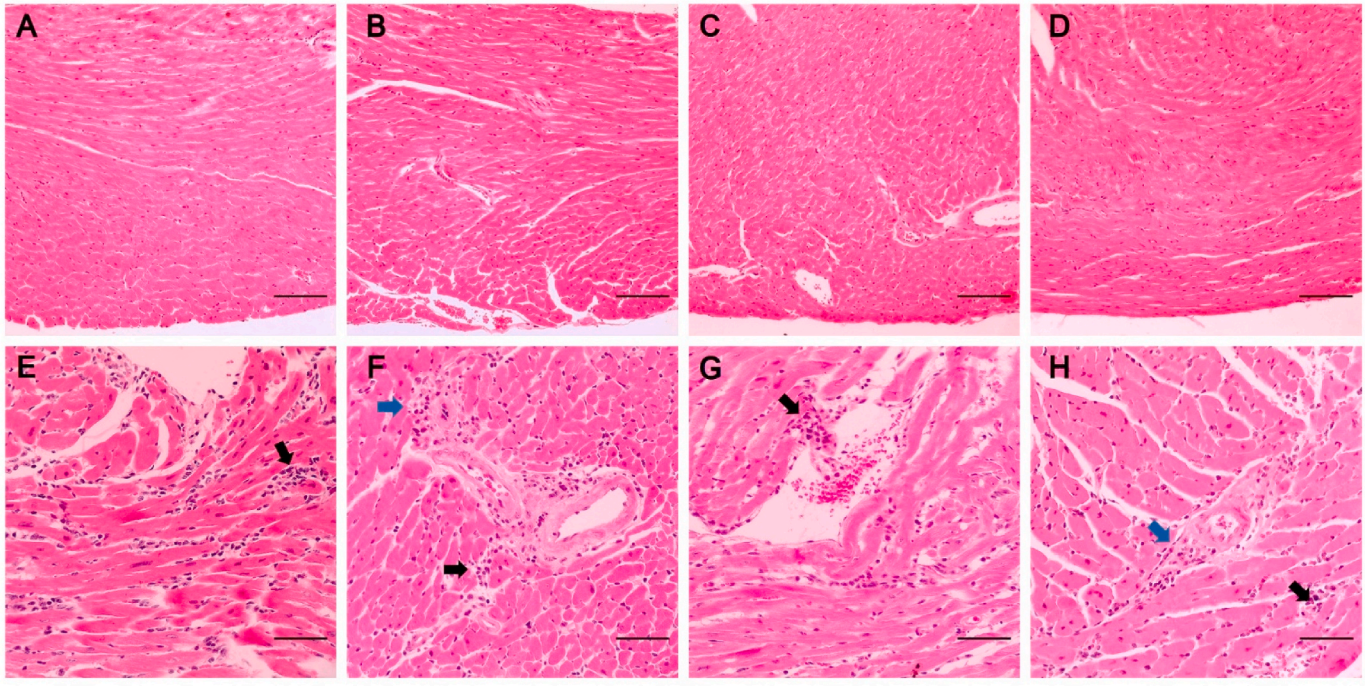

Fig. 4. Histological sections of the cardiac tissue of mice not infected and infected with *Trypanosoma cruzi* treated or not with erythropoietin. The upper panel shows images of the heart without changes in uninfected groups: 4A: Mouse from the NI_S_AP group; 4B: Mouse from the NI_S_CP group; 4C: Mouse from the NI_Epo_AP group, and 4D: Mouse from the NI_Epo_CP group. In the lower panel, changes in the cardiac tissue are observed in infected groups: 4E: Mouse from the I_S_AP group showing multifocal inflammatory infiltrate in the interstitial region (black arrow); 4F: Mouse from the I_S_CP group showing multifocal inflammatory infiltrates in the perivascular (blue arrow) and interstitial regions (black arrow); 4G: Mouse from the I_Epo_AP group showing multifocal inflammatory infiltrate in the interstitial region, and 4H: Mouse from the I_Epo_CP group showing multifocal inflammatory infiltrate in the perivascular (blue arrow) and interstitial regions (black arrow). H&E. Bars: 100 μm in the upper panel and 50 μm in the bottom panel. (For interpretation of the references to color in this figure legend, the reader is referred to the Web version of this article.)

antigens, hematological and biochemical parameters, Echo variables (EF, SF, and LVPWD), parasite load in distinct sites, and histological changes in these tissues was statistically analyzed. The results are shown in Fig. 5. The production of IgG against *T. cruzi* proteins was significantly positively correlated with several variables. Of note, antibody production was moderately associated with the parasite load in all analyzed tissues (blood, heart, spleen, and intestine) ($p < 0.003$), as well as with cardiomyocyte necrosis ($p = 0.003$) and inflammatory process in the intestine ($p = 0.002$) and in perivascular region of the heart ($p < 0.0001$). Higher production of anti-*T.cruzi* IgG was strongly associated with a more intense inflammatory process in the interstitial region of cardiac tissue ($p < 0.0001$). The anti-*T. cruzi* antibody production was positively correlated with some hematological parameters. Of note, a strong relationship was observed with the values of WBC ($p < 0.0001$) and absolute lymphocytes ($p < 0.0001$); a moderate correlation was seen with absolute monocytes ($p = 0.0002$) and segmented neutrophils ($p = 0.01$).

The cardiac parasite load was positively moderately associated with necrosis of cardiomyocytes ($p = 0.01$) and inflammatory process in the heart ($p < 0.0001$) and intestine ($p = 0.002$). The parasite burden in the spleen was not correlated with any histological changes, whilst blood parasitemia was only associated with inflammation in the intestine in a mild positive manner ($p = 0.03$). In turn, a weak positive correlation was observed between the number of parasites in the intestine and the inflammatory process in this tissue ($p = 0.04$), as well as in the interstitial region of the heart ($p = 0.03$), while in the perivascular region the association was moderate ($p = 0.0002$).

The inflammation of the intestine was directly associated with histological changes in the heart (necrosis, $p < 0.0001$; fibrosis, $p = 0.05$; and inflammatory process, $p < 0.0001$). Alterations in splenic tissue presented only a weak positive correlation with HGB ($p = 0.05$).

Regarding the Echo parameters, a very strong and directly proportional correlation was detected between EF and SF ($p < 0.0001$). On the other hand, both variables were negatively associated with Hct values (weak correlation, $p \leq 0.05$). Last, EF and SF were inversely associated with cardiac necrosis ($p \leq 0.03$) and inflammatory infiltrates in the cardiac interstitial region ($p \leq 0.04$).

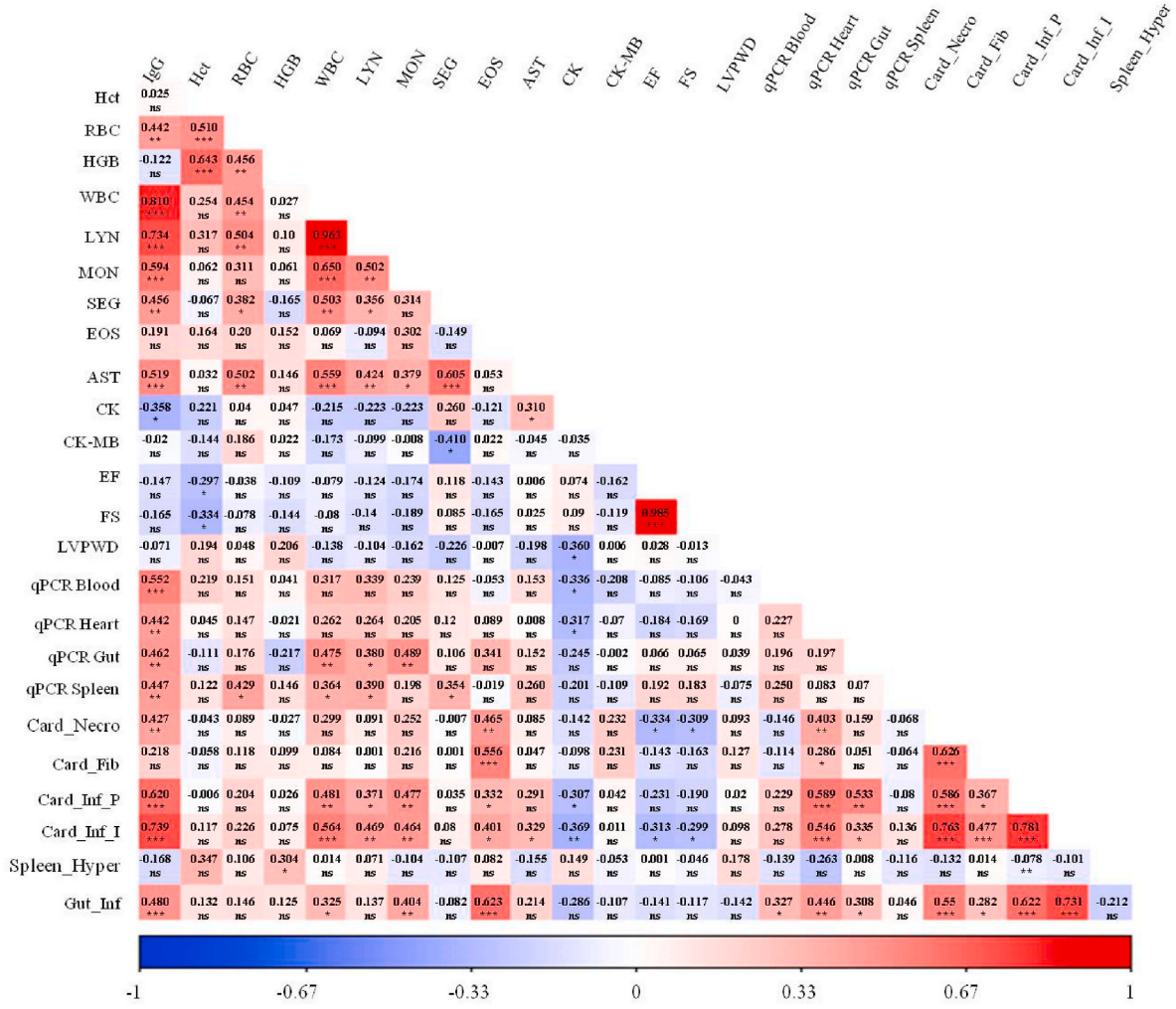

Fig. 5. Heat map with the correlation analysis between the different variables evaluated. The heat map shows the correlation of production of anti-*T. cruzi* antibodies (IgG), hematocrit (Hct), Red blood cells (RBC), hemoglobin concentration (HGB), white blood cells (WBC), lymphocytes (LYN), monocytes (MON), segmented neutrophils (SEG), eosinophils (EOS), aspartate aminotransferase (AST), total creatine kinase (CK), creatine kinase myocardial band (CK-MB), ejection fraction (EF), fractional shortening (FS), left ventricule posterior wall thickness in diastole (LVPWD), parasitemia (qPCR Blood), parasitic load in the heart (qPCR Heart), parasitic load in the large intestine (qPCR Gut), parasitic load in spleen (qPCR Spleen), cardiac necrosis (Card_Necro), cardiac fibrosis (Card_Fib), inflammatory infiltrate in the perivascular region of the heart (Card_Inf_P), inflammatory infiltrate in the interstitial region of the heart (Card_Inf_I), follicular hyperplasia in the spleen (Spleen_Hyper), inflammatory infiltrate in intestine (Gut_Inf). *$p < 0.05$, **$p < 0.01$, ***$p < 0.001$, ns: non significant. (For interpretation of the references to color in this figure legend, the reader is referred to the Web version of this article.)

4. Discussion

Beyond its effect on erythropoiesis, Epo has pleiotropic properties in several organs, including the heart (for review, see, Sølling, 2012). Here we investigated the outcomes of Epo administration in C57BL/6 mice during myotropic *T. cruzi* Colombian strain infection. To our knowledge, this is the first study that explores the role of Epo intervention in *T. cruzi* infection. Suzuki et al. administered Epo in a murine model infected with *Trypanosoma congolense* obtaining beneficial effects (Suzuki et al., 2006). However, in this case, the Epo-treatment was based on its hematopoietic action to compensate for the anemia, the key feature of the diseases caused by this protozoan (Noyes et al., 2009). Conversely, our study focuses on Epo's cardioprotective actions and its general effects on the organism of infected *T. cruzi* mice.

Although C57BL/6 mice are resistant to *T. cruzi*, this lineage infected with Colombian strain is a good model for studying the pathophysiology of Chagas disease and testing therapeutic drugs (Pereira et al., 2014). Since the infection of all our experimental animals lasted 180 days to ensure the establishment of the chronic phase of Chagas disease, we choose the C57BL/6 mice to guarantee a high survival rate during the study. However, our *T. cruzi* infected saline-mice did not exhibit cardiomegaly on macroscopic examination and only 20% of these animals had moderate or severe impairment in left ventricular function at 180 dpi evaluated by EF and cardiac fibrosis. These data indicate that chronic cardiac changes did not express the same degree of severity in mice model compared to human infections, even though 80% of infected animals showed interstitial cell infiltrates. Studies with humans had shown grossly enlarged hearts in patients who died with chronic Chagas disease in addition to chronic myocarditis, inflammatory infiltrates, and heart fibrosis (for review, see Acquatella, 2007). Indeed, human Chagas disease has a wide spectrum with respect to the severity of symptoms and cardiac clinical manifestations (for review, see Rassi et al., 2017).

A positive association between leukocyte number and parasitaemia has been suggested since *T. cruzi* infection should increase the production of defense cells (Villalba-Alemán et al., 2018). Here, WBC count did not significantly correlate positively with the number of *T. cruzi* in the blood or heart, but with the parasite load in the spleen and intestine (Fig. 5). Although hematological parameters are not strongly associate with histopathological alterations of Chagas disease (Villalba-Alemán et al., 2018), our results showed a significant positive correlation between the blood levels of WBC, lymphocytes, monocytes, and eosinophils, and heart inflammatory cell infiltrate (Fig. 5).

Regardless of *T. cruzi* infection, as expected, enhanced levels of Hct were seen after 30 days of Epo administration. HGB, in turn, remained elevated until the end of the experimental period in Epo-treated mice. Indeed, it is well known that Epo supplementation rises the Hct and HGB in humans (Christensen et al., 2011; Ekblom and Berglund, 1991; Lundby et al., 2007) and rodents (Coffey et al., 2018; Wang et al., 2018).

In healthy individuals, Lundby et al. reported no effect on the number of WBC with Epo treatment (Lundby et al., 2007). Indeed, in our study, the amount of WBC after 60 or 150 days of treatment (at d180) remained unchanged in all groups that received Epo, except for NI_Epo_CP, in which the number decreased after Epo supplementation (Table 2). Of note, the organism's response to Epo is influenced by dosage, type of administration, and frequency of administration (Tangri et al., 2011).

Since Epo has anti-inflammatory properties, it could be speculated that the number of WBC would decline in infected mice treated with this glycoprotein compared to uninfected ones. Meanwhile, in all infected Epo-treated animals, the amount, not only of WBC, but also of lymphocytes, segmented neutrophils, and eosinophils remained at the initial level. Only the absolute number of monocytes raised with chronic infection in mice submitted to Epo treatment. Noteworthy, the complete blood count was performed only at the beginning (d0) and the end of the study (180 days of infection). It would have been helpful to analyze more time points during the course of infection to obtain more valuable information and a better analysis of hematological changes caused by the *T. cruzi* associated with Epo administration. This was not done to avoid repeated mice blood collection.

Although in general AST serum activity suggests liver damage, it is also found in cardiac muscles (Dos Santos et al., 2020) and may indicate a lesion in this organ. Infected animals showed higher AST values than uninfected without a significant effect of Epo in this parameter (Table S1). As we did not analyze the liver, we cannot be sure whether the observed alterations in the serum activity of this enzyme represent a liver and/or heart injury. Nevertheless, necrosis, which is characterized by rupture of the plasma membrane and leakage of cellular content out of the cell (Leist and Jäättelä, 2001), was observed in heart sections of infected mice (Table 4). Likewise, infected mice had shown a greater amount of inflammatory infiltrate (Table 4 and Fig. 4) that induces cardiomyocyte damage (Silva et al., 2008) and fibrosis. Thus, cardiac damage could justify the increase in AST observed in infected mice.

In a rat model of sepsis-induced myocardial injury, Qin et al. used AST as a heart enzyme indicator and showed that six and 12 h after surgery inducing sepsis, AST levels decreased after the intervention of Epo. However, 24 h after the cecal ligation, Epo-treated and untreated groups had equivalent values (Qin et al., 2013). In our trial, no change in AST was observed over time in uninfected Epo-treated animals. When Epo was given in the acute phase of *T. cruzi* infection, the AST kinetics was different from animals that received saline. While in I_S_AP the AST levels at d15, d90, and d180 were similar, in I_Epo_AP group, AST kinetics was as follow: $d0 < d15 > d90 = d180$. We can hypothesize that when Epo is administrated in the early phase of infection (d0 to d30), this substance may protect the organs that release the AST in case of damage (liver and/or heart). When Epo was administrated in the chronic phase of infection, this possible effect was not seen. While the group I_S_CP presented the same time course of I_S_AP, in I_Epo_CP group levels of AST were similar at d15 to d180 which values were higher than d0 and d90 (Table 3).

It has been shown that Epo supplementation during 12 days did not alter serum CK levels in rats (Karthick et al., 2015). In accordance, CK values were unchanged with 15 days of Epo administration in our uninfected mice (NI_Epo_AP) (d0 compared to d15) (Table 3). In NI_Epo_CP, CK dosage was not performed in the initial days of treatment, this was only done 60 days after the end of Epo supplementation. Karthick et al. also showed that Epo administration retrieves the serum CK levels in rats with chronic renal failure, a condition that causes widespread damage to organs including cardiovascular problems (Karthick et al., 2015). Here, when the treatment was associated with the acute *T. cruzi* infection, at 15 dpi (i.e. 15 days of Epo administration), serum CK was higher than the baseline (Table 3). Thus, the maintenance of CK levels in infected mice that might suggest no cardiac damage was not seen with short-term treatment. It is worth highlighting that the CK presented a high variability intra and inter-group, making definitive conclusions difficult. Variations like that were also found in De Souza et al. (De Souza et al., 2000). The high variability may be due to hemolysis resulting from retro-orbital blood collection (Mazzaccara et al., 2008).

After the important increase in CK serum levels with 15 days of infection in the I_Epo_AP group, the values decreased on d90 and d180 (i.e. 60 and 150 after the end of treatment), although at these times the CK remained higher than d0 (Table 3). Evaluation of CK after 180 days of infection would be necessary to verify if early treatment with Epo has long-term effects on CK activity since after a large increase at d15, the levels have dropped. If on the one hand, the effects of early treatment with Epo in infected mice could not be proven by the CK measure, administration in the chronic phase (I_Epo_CP group), when cardiac lesions usually appear, seems to be more interesting, since the CK levels have not changed over time. Most histological results corroborate this idea since no heart necrosis or fibrosis was seen in I_Epo_CP contrary to I_Epo_AP group. The latter also tended to have more inflammatory infiltrates in the perivascular region of cardiac tissue (Table 4).

CK-MB has been reported as a highly specific biomarker of cardiac

injury (Adams et al., 1993). Elevated levels of CK-MB were observed in left ventricular hypertrophy (Adams et al., 1993) and it was considered a relevant non-invasive indicator of heart damage in both acute (Carvalho et al., 2012; De Souza et al., 2000; Kroll-Palhares et al., 2008) and chronic phases of experimental Chagas disease (Carvalho et al., 2012; Medeiros et al., 2009; Pereira et al., 2014). A large individual variation in the activity of this enzyme was observed by Zhou and Hansson (2004) in uninfected mice and by Soares et al. (2012) in *T. cruzi* infected ones. The lasted authors reported higher CK-MB activity in mice with Chagas disease, as Pereira et al. showed an increase of CK-MB in chronically *T. cruzi* infected mice (Pereira et al., 2014). Our data did not show an effect of infection alone on CK-MB levels, despite the significant effect of infection on cardiac necrosis and fibrosis seen in histological analysis.

Furthermore, the kinetics of CK-MB in each group showed that regardless of *T. cruzi* infection, the chronic Epo administration reduced CK-MB serum activity from d0 to d180, suggesting a general beneficial effect of Epo and perhaps a reduction in myocardial damage in infected animals. This decrease in CK-MB levels was not observed in animals Epo-treated in the acute phase (Table 3). As heart lesions due to Chagas disease usually appear in the chronic phase, it seems that Epo is unable to prevent myocardial damage when administered before the emergence of lesions ruling out a possible protective effect of Epo in Chagas cardiomyopathy. On the other hand, when administered in the chronic phase, when heart problems may occur, Epo seems to have a positive therapeutic effect that needs to be further studied. Although statistical differences in histological exams were not found between infected groups treated with Epo in acute or chronic phase, the former tended to have a greater number of cardiac alterations (e.g. necrosis, fibrosis, and inflammation perivascular was observed in 28.6%, 14.3%, and 71.4% of I_Epo_AP animals compared to 0% for the first two variables and 37% for the last one in I_Epo_CP group) (Table 4). As mentioned before, Epo has a cardioprotective action in many situations. Gholamzadeh et al., for example, reported that a high dose of Epo administrated after percutaneous coronary intervention in patients with myocardial infarction did not modify the level of CK-MB 24 h after the angioplasty (Gholamzadeh et al., 2015).

Intracellular parasite nests were found in only one heart mouse from I_S_AP group at 180 dpi. In fact, parasites detection using histology has been found only in rare chronically infected mouse models (Marinho et al., 2004). Using Balb/c mice chronically infected with *T. cruzi*, Wesley et al. did not visually detect amastigote nests in cardiac tissue of animals infected with CL Brener and Y strains (Wesley et al., 2019). However, parasite nests were seen in 40% of infected mice with Colombian strain. In mice with chronic Chagas cardiomyopathy, histopathological heart analysis showed scarce tissue parasitism, despite the presence of infiltrating inflammatory, fibrosis, hypertrophy, and myocarditis (Scarim et al., 2018). Similar to our study, no amastigote nests were found by Wesley et al. (2019) in the intestine of any animal.

Although amastigotes nests were barely observed, parasite DNA was detected by qPCR in all the tissues evaluated of infected mice (Fig. 3). In fact, the qPCR assays are more sensitive than histology, even though the latter allows the recognition of parasites *in situ*. Thus, very scarce amastigote might be present in some tissues, but they are below the level of detection under light microscope. Bioluminescence studies have been demonstrated the dynamics of *T. cruzi* that can move from one tissue to another in chronically infected mice (Lewis et al., 2014; Silberstein et al., 2018). Indirectly, our qPCR results support this idea, although this technique does not differentiate between live and dead parasites (Jimenez-Marco et al., 2017) and may not represent the real parasite localization. Despite that, our qPCR data suggested the parasite persistence in chronically infected mice mainly in blood, heart, and intestine (Fig. 3). Yet, the spleen appears to remain infected according to qPCR results of Silberstein et al. who found *T. cruzi* in this tissue during the chronic infection with Colombiana strain, even if in low quantities (Silberstein et al., 2018). Of note, in blood and intestine, the quantification of parasite DNA showed discrepant concentrations in some mice (Fig. 3). The variation in parasite load between animals was also observed by Rodrigues-dos-Santos et al. (Rodrigues-dos-Santos et al., 2018) and Wesley et al. (2019).

Even though the *T. cruzi* strain used in this work was the myotropic Colombian which preferably infect cardiomyocytes and not a reticulotropic strain, in which parasites are most commonly found in the spleen and liver (Erdmann et al., 2016), the spleen was analyzed since it was observed its enlargement and due to its important immunological function. Regarding the *T. cruzi* DNA levels in the spleen, it was remarkably low but higher than the detection limit of our qPCR method (i.e. 0.001 par.eq./30 ng total DNA) (Fig. 3). Nevertheless, as the spleen is an extremely vascularized organ, the parasite load found may be that of the blood present in the tissue. In their review, Lewis and Kelly discuss this limit of the qPCR technique that can lead to misinterpretation about the location of *T. cruzi* in some tissues (Lewis and Kelly, 2016).

Lewis et al., using the bioluminescence showed that the spleen was highly parasitized in the acute phase of infected mice (Lewis et al., 2018). Using *ex vivo* image, Silberstein et al. did not detect parasites in the spleen in chronically infected mice, despite having demonstrated low parasite load by qPCR and that the mass of this organ was three times greater than in uninfected mice (Silberstein et al., 2018). The splenomegaly which is frequently observed in experimental *T. cruzi* infection (Francisco et al., 2015; Jelicks and Tanowitz, 2011; Scarim et al., 2018; Silverio et al., 2012) and reported in some human patients (Jelicks and Tanowitz, 2011), was also observed in our infected animals. Actually, this organ is involved in immune response and as a result, in many diseases, an increase in its size is observed (Eichner, 1979).

Our results showed follicular hyperplasia in the splenic white pulp possibly related to the immunostimulation in infected mice, Epo-treated or not. On the other hand, Epo treated animals, infected or not, showed twice as many splenic changes compared to untreated mice. A likely explanation for this is the fact that the spleen of mice treated with Epo may have been overwhelmed since in this species, in contrast to humans, the spleen is also a site for erythropoiesis (Bozzini et al., 1970; Brodsky et al., 1966) and may overshadow the bone-marrow when a marked erythropoietic stimulus is present (Bozzini et al., 1970; Marsh et al., 1968). Thereby, without infection, but with the administration of Epo, the enlarged spleen may be a result of higher organ requirement due to the hemodynamic modification (e.g. destruction of a greater amount of red blood cells). However, if this happened, there was no impact on cardiac tissue, as shown in the histological analysis.

Besides the spleen, our qPCR results revealed that the blood, heart, and large intestine remain infected during the chronic infection with *T. cruzi*. Of note, Epo did not alter the number of circulating parasites (Fig. 3).

The anti-apoptotic (Burger et al., 2006, 2009) and anti-inflammatory (Burger et al., 2009; Li et al., 2006; Rui et al., 2005) role of Epo in the myocardium is well documented in models without *T. cruzi* infection. In our study, Epo provided acutely or chronically did not effectively reduce heart parasitism (Fig. 3) or inflammation, however, cardiac necrosis and fibrosis tended to decrease (Table 4).

Myocardial fibrosis is a common clinical finding in patients with chronic Chagas cardiomyopathy (Ferreira et al., 2019; Martinez et al., 2019). Differences in cardiac fibrosis detected between mice injected with saline in the acute and chronic phase of infection do not enable a definitive conclusion and could be related to distinct individual susceptibility (Table 4). When we look at the results of qPCR, the number of parasites in the heart was higher in the I_S_CP than I_S_AP (Fig. 3). The parasite persistence influences the clinical outcome of the infection allowing cardiac damage. Actually, the correlation analysis showed that the higher parasite load in the heart was linked to cardiac inflammation and necrosis (Fig. 5) reinforcing the parasite persistence theory which affirms that the presence of *T. cruzi* is the responsible for maintenance of chronic inflammation and tissue damage (Cruz et al., 2016). However, it is important to emphasize that other theories based on the host's autoimmune reactions try to explain the pathogenesis of Chagas disease,

which until now has not been well established (De Bona et al., 2018).

The antibody production against *T. cruzi* was positively correlated with several of the analyzed parameters (Fig. 5). Indeed, anti-*T. cruzi* IgG antibodies have been associated with Chagas disease progression (Santos et al., 2012; Zauza and Borges-Pereira, 2001) and might be related to the clinical outcome (Georg et al., 2017; Santos et al., 2012; Buss et al., 2020). In this work, an important correlation between the production of IgG against *T. cruzi* and the parasitemia and parasite load in heart, large intestine, and spleen was detected, suggesting that the humoral immune response to *T. cruzi* infection is consistent with the parasite persistence. In a cohort of humans with Chagas disease, the connection between *T. cruzi* specific antibodies and blood PCR positivity was also observed by Buss et al. (Buss et al., 2020). In rodents, Wesley et al. found that a higher parasite burden in the heart was not significantly correlated with antibody levels against *T. cruzi*, while an association of antibody production with intestinal parasite load was observed (Wesley et al., 2019).

The antibody production influences inflammatory cell infiltration in tissues (Wesley et al., 2019). In fact, anti-*T. cruzi* antibodies levels were directly associated with a higher degree of inflammatory process in the heart and intestine, in addition to cardiomyocyte necrosis.

Since Echo is a valuable non-invasive technique to assess cardiac structure and function in mice (Collins et al., 2003; Syed et al., 2005), a useful tool for monitoring cardiac dysfunction in these rodents (Fayssoil, 2008; Lindsey et al., 2018; Moran et al., 2013; Stypmann et al., 2009), and makes possible to assess the response to therapeutic interventions, we use this method to evaluate if Epo ameliorates the progression of heart Chagas disease. In addition, Chandra et al. underscore the utility of Echo in murine model of Chagas disease that also allows serial examinations on the same animal (Chandra et al., 2002).

Both FS and EF are good parameters for assessing left ventricular systolic function (Syed et al., 2005). In murine, there is a wide range of reported values for the different variables measured by Echo. Vinhas et al. provide reference values in adults 129/Sv mice under isoflurane anesthesia (Vinhas et al., 2013). However, since Echo measurements are influenced by the lineage of mice, age, sex, and regimen of anesthesia (Collins et al., 2003), we considered a series of studies to average the values of FS and EF. A total of nine studies (Bai et al., 2016; Collins et al., 2001; Du et al., 2016; Esporcatte et al., 2010; Esposito et al., 2000; Stypmann et al., 2006; Vinhas et al., 2013; Xu et al., 2016; Yang et al., 1999) in healthy mice under anesthesia have shown FS mean value of 38.37% ± 5.98. Four of them (Bai et al., 2016; Du et al., 2016; Vinhas et al., 2013; Yang et al., 1999) plus Takawale et al. (2014) also measured the EF which showed a mean value of 65.70% ± 8.52. At d180, only the I_Epo_AP group had impaired left ventricular systolic function considering the mean values of FS and EF (Fig. S1) established by the aforementioned studies. This result suggests that Epo treatment may be harmful in the long run when administered in the acute phase of *T. cruzi* infection, while treatment in the chronic phase restored the cardiac function. Actually, there was a trend towards greater EF and FS in I_Epo_CP group than in the controls. The analysis of cardiac involvement using the human parameters of EF corroborates this idea since the I_Epo_CP was the only infected group with 100% of animals with EF above 55% corresponding to the absence of cardiac damage (Fig. 2). This was confirmed by the thickness of the posterior LV wall in systole (LVPWS) and histological analysis.

5. Conclusions

We tested whether Epo administration could protect the heart of an organism infected with *T. cruzi*. Epo has no anti-parasitic activity at the tested concentrations, however, an overall reduction in cardiac alterations could be seen. The analysis of biochemical dosages and echocardiographic data suggest a possible effect of Epo when administered in the chronic phase of Chagas disease. The optimal dosage, timing, and frequency of Epo intervention to induce heart protection and reduce inflammation in *T. cruzi* infection need to be further clarified. Alternative schedules should be investigated, including combined treatment with benznidazole, the trypanocid drug most employed in Chagas disease treatment, since the therapeutic activity of the medicine association may be superior to that of an isolated substance. In conclusion, our findings provide the first evidence about the possible contribution of the Epo, even if subtle, in a murine model of experimental *T. cruzi* infection. A more complete understanding would require further studies.

Funding

This work was supported by the Fundação de Apoio a Pesquisa do Distrito Federal (FAPDF) (grant number 193.000.666/2015) and Coordenação de Aperfeiçoamento de Pessoal de Nível Superior (88882.384138/2019-01).

Authors contributions

L.H and B.D conceived and planned the experiments. A.C.C.N and L. H. participated in all experiments. C.F.P and G.M.S.R. performed some of the experiments. G.R.P was responsible for the biochemical analysis, G.B.P.N for echocardiography, and M.B.C for histopathology. M.M., N. N, B.D, and L.H. contributed to the analysis and interpretation of data. L. H took the lead in writing the manuscript. N.N, M.M, and B.D helped shape the final report. All authors read and approved the final manuscript.

Declaration of competing interest

The authors declare that there is no conflict of interest.

Appendix A. Supplementary data

Supplementary data related to this article can be found at https://doi.org/10.1016/j.ijpddr.2022.05.005.

References

Acquatella, H., 2007. Echocardiography in Chagas heart disease. Circulation 115, 1124–1131. https://doi.org/10.1161/CIRCULATIONAHA.106.627323.

Adams, J.E., Abendschein, D.R., Jaffe, A.S., 1993. Biochemical markers of myocardial injury: is MB creatine kinase the choice for the 1990s? Circulation 88, 750–763. https://doi.org/10.1161/01.cir.88.2.750.

Bai, T., Hu, X., Zheng, Y., Wang, S., Kong, J., Cai, L., 2016. Resveratrol protects against lipopolysaccharide-induced cardiac dysfunction by enhancing SERCA2a activity through promoting the phospholamban oligomerization. Am. J. Physiol. Heart Circ. Physiol. 311, H1051–H1062. https://doi.org/10.1152/ajpheart.00296.2016.

Bern, C., 2015. Chagas' disease. N. Engl. J. Med. 373 https://doi.org/10.1056/NEJMra1410150.

Bocchi, E.A., Bestetti, R.B., Scanavacca, M.I., Cunha Neto, E., Issa, V.S., 2017. Chronic chagas heart disease management: from etiology to cardiomyopathy treatment. J. Am. Coll. Cardiol. 70, 1510–1524. https://doi.org/10.1016/j.jacc.2017.08.004.

Bozzini, C.E., Barrio Rendo, M.E., Devoto, F.C., Epper, C.E., 1970. Studies on medullary and extramedullary erythropoiesis in the adult mouse. Am. J. Physiol. 219, 724–728. https://doi.org/10.1152/ajplegacy.1970.219.3.724.

Brener, Z., 1962. Therapeutic activity and criterion of cure on mice experimentally infected with Trypanosoma cruzi. Rev. Inst. Med. Trop. 4, 389–396.

Brodsky, I., Dennis, L.H., Kahn, S.B., Brady, L.W., 1966. Normal mouse erythropoiesis I. The role of the spleen in mouse erythropoiesis. Cancer Res. 26, 198–201.

Burger, D., Lei, M., Geoghegan-Morphet, N., Lu, X., Xenocostas, A., Feng, Q., 2006. Erythropoietin protects cardiomyocytes from apoptosis via up-regulation of endothelial nitric oxide synthase. Cardiovasc. Res. 72, 51–59. https://doi.org/10.1016/j.cardiores.2006.06.026.

Burger, D., Xenocostas, A., Feng, Q., 2009. Molecular basis of cardioprotection by erythropoietin. Curr. Mol. Pharmacol. 2, 56–69. https://doi.org/10.2174/1874467210902010056.

Buss, L.F., Campos de Oliveira-da Silva, L., Moreira, C.H.V., Manuli, E.R., Sales, F.C., Morales, I., Di Germanio, C., de Almeida-Neto, C., Bakkour, S., Constable, P., Pinto-Filho, M.M., Ribeiro, A.L., Busch, M., Sabino, E.C., 2020. Declining antibody levels to trypanosoma cruzi correlate with polymerase chain reaction positivity and electrocardiographic changes in a retrospective cohort of untreated Brazilian blood donors. PLoS Neglected Trop. Dis. 14, 1–14. https://doi.org/10.1371/journal.pntd.0008787.

Cançado, J.R., 2002. Long term evaluation of etiological treatment of Chagas disease with benznidazole. Rev. Inst. Med. Trop. Sao Paulo 44, 29–37. https://doi.org/10.1590/S0036-46652002000100006.

Carvalho, C.M.E., Silverio, J.C., da Silva, A.A., Pereira, I.R., Coelho, J.M.C., Britto, C.C., Moreira, O.C., Marchevsky, R.S., Xavier, S.S., Gazzinelli, R.T., da Bonecini-Almeida, M.G., Lannes-Vieira, J., 2012. Inducible nitric oxide synthase in heart tissue and nitric oxide in serum of Trypanosoma cruzi-infected rhesus monkeys: association with heart injury. PLoS Neglected Trop. Dis. 6 https://doi.org/10.1371/journal.pntd.0001644.

Castro-Sesquen, Y.E., Gilman, R.H., Yauri, V., Angulo, N., Verastegui, M., Velásquez, D. E., Sterling, C.R., Martin, D., Bern, C., 2011. Cavia porcellus as a model for experimental infection by trypanosoma cruzi. Am. J. Pathol. 179, 281–288. https://doi.org/10.1016/j.ajpath.2011.03.043.

Cevey, Á.C., Mirkin, G.A., Donato, M., Rada, M.J., Penas, F.N., Gelpi, R.J., Goren, N.B., 2017. Treatment with Fenofibrate plus a low dose of Benznidazole attenuates cardiac dysfunction in experimental Chagas disease. Int. J. Parasitol. Drugs Drug Resist. 7, 378–387. https://doi.org/10.1016/j.ijpddr.2017.10.003.

Chandra, M., Shirani, J., Shtutin, V., Weiss, L.M., Factor, S.M., Petkova, S.B., Rojkind, M., Dominguez-Rosales, J.A., Jelicks, L.A., Morris, S.A., Wittner, M., Tanowitz, H.B., 2002. Cardioprotective effects of verapamil on myocardial structure and function in a murine model of chronic Trypanosoma cruzi infection (Brazil Strain): an echocardiographic study. Int. J. Parasitol. 32, 207–215. https://doi.org/10.1016/S0020-7519(01)00320-4.

Christensen, B., Sackmann-Sala, L., Cruz-Topete, D., Jørgensen, J.O.L., Jessen, N., Lundby, C., Kopchick, J.J., 2011. Novel serum biomarkers for erythropoietin use in humans: a proteomic approach. J. Appl. Physiol. 110, 149–156. https://doi.org/10.1152/japplphysiol.00665.2010.

Coffey, R., Sardo, U., Kautz, L., Gabayan, V., Nemeth, E., Ganz, T., 2018. Erythroferrone is not required for the glucoregulatory and hematologic effects of chronic erythropoietin treatment in mice. Phys. Rep. 6 https://doi.org/10.14814/phy2.13890.

Collins, K.A., Korcarz, C.E., Lang, R.M., 2003. Use of echocardiography for the phenotypic assessment of genetically altered mice. Physiol. Genom. 13, 227–239. https://doi.org/10.1152/physiolgenomics.00005.2003.

Collins, K.A., Korcarz, C.E., Shroff, S.G., Bednarz, J.E., Fentzke, R.C., Lin, H., Leiden, J. M., Lang, R.M., 2001. Accuracy of echocardiographic estimates of left ventricular mass in mice. Am. J. Physiol. Heart Circ. Physiol. 280 https://doi.org/10.1152/ajpheart.2001.280.5.h1954, 1954–1962.

Coura, J.R., Borges-Pereira, J., 2010. Chagas disease: 100 years after its discovery. A systemic review. Acta Trop. 115, 5–13. https://doi.org/10.1016/j.actatropica.2010.03.008.

Cruz, J.S., Santos-Miranda, A., Sales, P.A., Monti-Rocha, R., Campos, P.P., Machado, F.S., Roman-Campos, D., 2016. Altered cardiomyocyte function and Trypanosoma cruzi persistence in Chagas disease. Am. J. Trop. Med. Hyg. 94, 1028–1033. https://doi.org/10.4269/ajtmh.15-0255.

Cunha-Neto, E., Chevillard, C., 2014. Chagas disease cardiomyopathy: immunopathology and genetics. Mediat. Inflamm. https://doi.org/10.1155/2014/683230, 2014.

De Bona, E., Lidani, K.C.F., Bavia, L., Omidian, Z., Gremski, L.H., Sandri, T.L., de Messias Reason, I.J., 2018. Autoimmunity in chronic chagas disease: a road of multiple pathways to cardiomyopathy? Front. Immunol. 9, 1–8. https://doi.org/10.3389/fimmu.2018.01842.

De Souza, A.P., Olivieri, B.P., De Castro, S.L., Araújo-Jorge, T.C., 2000. Enzymatic markers of heart lesion in mice infected with Trypanosoma cruzi and submitted to benznidazole chemotherapy. Parasitol. Res. 86, 800–808. https://doi.org/10.1007/s004360000262.

Dias, J.P., Bastos, C., Araújo, E., Mascarenhas, A.V., Netto, E.M., Grassi, F., Silva, M., Tatto, E., Mendonça, J., Araújo, R.F., Shikanai-Yasuda, M.A., Aras, R., 2008. Acute Chagas disease outbreak associated with oral transmission. Rev. Soc. Bras. Med. Trop. 41, 296–300. https://doi.org/10.1590/S0037-86822008000300014.

Dos Santos, V.R.C., Antunes, D., de Souza, D.D.S.M., Moreira, O.C., de A Lima, I.C., Farias-De-oliveira, D.A., Lobo, J.P., de Meis, E., Coura, J.R., Savino, W., Junqueira, A.C.V., de Meis, J., 2020. Human acute chagas disease: changes in factor vii, activated protein C and hepatic enzymes from patients of oral outbreaks in pará state (Brazilian Amazon). Mem. Inst. Oswaldo Cruz 115, 1–6. https://doi.org/10.1590/0074-02760190364.

Du, J., Zhang, L., Wang, Z., Yano, N., Zhao, Y.T., Wei, L., Dubielecka-Szczerba, P., Liu, P. Y., Zhuang, S., Qin, G., Zhao, T.C., 2016. Exendin-4 induces myocardial protection through MKK3 and Akt-1 in infarcted hearts. Am. J. Physiol. Cell Physiol. 310, C270–C283. https://doi.org/10.1152/ajpcell.00194.2015.

Eichner, E.R., 1979. Splenic function: normal, too much and too little. Am. J. Med. 66, 311–320. https://doi.org/10.1016/0002-9343(79)90554-0.

Ekblom, B., Berglund, B., 1991. Effect of erythropoietin administration on mammal aerobic power. Scand. J. Med. Sci. Sports 1, 88–93. https://doi.org/10.1111/j.1600-0838.1991.tb00276.x.

El Hasnaoui-Saadani, R., Marchant, D., Pichon, A., Escoubet, B., Pezet, M., Hilfiker-Kleiner, D., Hoch, M., Pham, I., Quidu, P., Voituron, N., Journé, C., Richalet, J.P., Favret, F., 2013. Epo deficiency alters cardiac adaptation to chronic hypoxia. Respir. Physiol. Neurobiol. 186, 146–154. https://doi.org/10.1016/j.resp.2013.01.003.

Erdmann, H., Behrends, J., Hölscher, C., 2016. During acute experimental infection with the reticulotropic Trypanosoma cruzi strain Tulahuen IL-22 is induced IL-23-dependently but is dispensable for protection. Sci. Rep. 6, 1–13. https://doi.org/10.1038/srep32927.

Esporcatte, B.L.B., Rocha, N.N., Mello, D.B., Dutra, K., Lachtermacher, S., Coeli, R., Carlos, A., De Carvalho, C., 2010. Ecocardiograma de Alta Resolução e o Modelo de Infarto do Miocárdio em Camundongos High Resolution Echocardiography and the Myocardial Infarction Model in Mice causa de mortalidade no Brasil , segundo o banco o desenvolvimento de novas terapias. Que Poss 23, 18–24.

Esposito, G., Santana, L.F., Dilly, K., Cruz, J., dos, S., Mao, L., Lederer, W.J., Rockman, H. A., 2000. Cellular and functional defects in a mouse model of heart failure. Am. J. Physiol. Heart Circ. Physiol. 279, H3101–H3112. https://doi.org/10.1152/ajpheart.2000.279.6.H3101.

Fayssoil, A., 2008. Échocardiographie de La souris. Ann. Cardiol. Angeiol 57, 177–180. https://doi.org/10.1016/j.ancard.2008.05.004.

Ferreira, R.R., Abreu, R. da S., Vilar-Pereira, G., Degrave, W., Meuser-Batista, M., Ferreira, N.V.C., da Cruz Moreira, O., da Silva Gomes, N.L., Mello de Souza, E., Ramos, I.P., Bailly, S., Feige, J.J., Lannes-Vieira, J., de Araújo-Jorge, T.C., Waghabi, M.C., 2019. TGF-β inhibitor therapy decreases fibrosis and stimulates cardiac improvement in a pre-clinical study of chronic Chagas' heart disease. PLoS Neglected Trop. Dis. 13, 1–27. https://doi.org/10.1371/journal.pntd.0007602.

Francisco, A.F., Lewis, M.D., Jayawardhana, S., Taylor, M.C., Chatelain, E., Kelly, J.M., 2015. Limited ability of posaconazole to cure both acute and chronic Trypanosoma cruzi infections revealed by highly sensitive in vivo imaging. Antimicrob. Agents Chemother. 59, 4653–4661. https://doi.org/10.1128/AAC.00520-15.

Franco-Paredes, C., Villamil-Gómez, W.E., Schultz, J., Henao-Martínez, A.F., Parra-Henao, G., Rassi, A., Rodríguez-Morales, A.J., Suarez, J.A., 2020. A deadly feast: elucidating the burden of orally acquired acute Chagas disease in Latin America – public health and travel medicine importance. Trav. Med. Infect. Dis. 36, 101565 https://doi.org/10.1016/j.tmaid.2020.101565.

Georg, Ingebourg, Hasslocher-Moreno, Alejandro Marcel, Xavier, Sergio Salles, de Holanda, Marcelo Teixeira, Bonecini-Almeida, Maria da Gloria, 2017. Evolution of anti-*Trypanosoma cruzi* antibody production in patients with chronic Chagas disease: Correlation between antibody titers and development of cardiac disease severity. PLoS Negl. Trop. Dis. 11 (17), 1–22. doi:10.1371/journal.pntd.0005796.

Gholamzadeh, A., Amini, S., Mohammadpour, A.H., Vahabzadeh, M., Fazelifar, A.F., Fazlinezhad, A., Dehghani, M., Moohebati, M., Dastani, M., Malaekeh-Nikouie, B., Falsoleiman, H., 2015. Erythropoietin reduces post-PCI arrhythmias in patients with ST-elevation myocardial infarction. J. Cardiovasc. Pharmacol. 65, 555–561. https://doi.org/10.1097/FJC.0000000000000223.

Hagström, L., Agbulut, O., El-Hasnaoui-Saadani, R., Marchant, D., Favret, F., Richalet, J. P., Beaudry, M., Launay, T., 2010. Epo is relevant neither for microvascular formation nor for the new formation and maintenance of mice skeletal muscle fibres in both normoxia and hypoxia. J. Biomed. Biotechnol. https://doi.org/10.1155/2010/137817, 2010.

He, Q., Cheng, J., Wang, Y., 2019. Chronic CaMKII inhibition reverses cardiac function and cardiac reserve in HF mice. Life Sci. 219, 122–128. https://doi.org/10.1016/j.lfs.2019.01.010.

Hecht, M.M., Nitz, N., Araujo, P.F., Sousa, A.O., Rosa, A.D.C., Gomes, D.A., Leonardecz, E., Teixeira, A.R.L., 2010. Inheritance of DNA transferred from American trypanosomes to human hosts. PLoS One 5. https://doi.org/10.1371/journal.pone.0009181.

Jelicks, L.A., Tanowitz, H.B., 2011. Advances in imaging of animal models of chagas disease. Adv. Parasitol. 75, 193–208. https://doi.org/10.1016/B978-0-12-385863-4.00009-5.

Jimenez-Marco, T., Cancino-Faure, B., Girona-Llobera, E., Alcover, M.M., Riera, C., Fisa, R., 2017. The effectiveness of riboflavin and ultraviolet light pathogen reduction technology in eliminating Trypanosoma cruzi from leukoreduced whole blood. Transfusion 57, 1440–1447. https://doi.org/10.1111/trf.14071.

Karthick, N., D, A., Kn, P., C, V., S, A., B, D., Venkataraman, P., 2015. Neurobehavioral alterations and brain creatine kinase system changes in chronic renal failure induced male wistar rats: impact of erythropoietin supplementation. J. Bioequiv. Availab. 7 https://doi.org/10.4172/jbb.1000218.

Kroll-Palhares, K., Silvério, J.C., Da Silva, A.A., Michailowsky, V., Marino, A.P., Silva, N. M., Carvalho, C.M.E., Pinto, L.M.D.O., Gazzinelli, R.T., Lannes-Vieira, J., 2008. TNF/TNFR1 signaling up-regulates CCR5 expression by CD8+ T lymphocytes and promotes heart tissue damage during Trypanosoma cruzi infection: beneficial effects of TNF-α blockade. Mem. Inst. Oswaldo Cruz 103, 375–385. https://doi.org/10.1590/S0074-02762008000400011.

Lang, R.M., Bierig, M., Devereux, R.B., Flachskampf, F.A., Foster, E., Pellikka, P.A., Picard, M.H., Roman, M.J., Seward, J., Shanewise, J.S., Solomon, S.D., Spencer, K.T., St John Sutton, M., Stewart, W.J., 2005. Recommendations for chamber quantification: a report from the American Society of Echocardiography's guidelines and standards committee and the Chamber Quantification Writing Group, developed in conjunction with the European Association of Echocardiograph. J. Am. Soc. Echocardiogr. 18, 1440–1463. https://doi.org/10.1016/j.echo.2005.10.005.

Latini, R., Brines, M., Fiordaliso, F., 2008. Do non-hemopoietic effects of erythropoietin play a beneficial role in heart failure? Heart Fail. Rev. 13, 415–423. https://doi.org/10.1007/s10741-008-9084-z.

Launay, T., Hagström, L., Lottin-Divoux, S., Marchant, D., Quidu, P., Favret, F., Duvallet, A., Darribère, T., Richalet, J.P., Beaudry, M., 2010. Blunting effect of hypoxia on the proliferation and differentiation of human primary and rat L6 myoblasts is not counteracted by Epo. Cell Prolif 43. https://doi.org/10.1111/j.1365-2184.2009.00648.x.

Leist, M., Jäättelä, M., 2001. Four deaths and a funeral: from caspases to alternative mechanisms. Nat. Rev. Mol. Cell Biol. 2, 589–598. https://doi.org/10.1038/35085008.

Lewis, M.D., Fortes Francisco, A., Taylor, M.C., Burrell-Saward, H., Mclatchie, A.P., Miles, M.A., Kelly, J.M., 2014. Bioluminescence imaging of chronic Trypanosoma cruzi infections reveals tissue-specific parasite dynamics and heart disease in the absence of locally persistent infection. Cell Microbiol. 16, 1285–1300. https://doi.org/10.1111/cmi.12297.

Lewis, M.D., Francisco, A.F., Jayawardhana, S., Langston, H., Taylor, M.C., Kelly, J.M., 2018. Imaging the development of chronic Chagas disease after oral transmission. Sci. Rep. 8, 1–8. https://doi.org/10.1038/s41598-018-29564-7.

Lewis, M.D., Kelly, J.M., 2016. Putting infection dynamics at the heart of chagas disease. Trends Parasitol. 32, 899–911. https://doi.org/10.1016/j.pt.2016.08.009.

Li, Y., Takemura, G., Okada, H., Miyata, S., Maruyama, R., Li, L., Higuchi, M., Minatoguchi, S., Fujiwara, T., Fujiwara, H., 2006. Reduction of inflammatory cytokine expression and oxidative damage by erythropoietin in chronic heart failure. Cardiovasc. Res. 71, 684–694. https://doi.org/10.1016/j.cardiores.2006.06.003.

Lindsey, M.L., Kassiri, Z., Virag, J.A.I., De Castro Brás, L.E., Scherrer-Crosbie, M., 2018. Guidelines for measuring cardiac physiology in mice. Am. J. Physiol. Heart Circ. Physiol. 314, H733–H752. https://doi.org/10.1152/ajpheart.00339.2017.

Lombardero, M., Kovacs, K., Scheithauer, B.W., 2011. Erythropoietin: a hormone with multiple functions. Pathobiology 78, 41–56. https://doi.org/10.1159/000322975.

Longhi, S.A., Brandariz, S.B., Lafon, S.O., Niborski, L.L., Luquetti, A.O., Schijman, A.G., Levin, M.J., Gómez, K.A., 2012. Evaluation of in-house ELISA using Trypanosoma cruzi lysate and recombinant antigens for diagnosis of chagas disease and discrimination of its clinical forms. Am. J. Trop. Med. Hyg. 87, 267–271. https://doi.org/10.4269/ajtmh.2012.11-0533.

Lu, J., Yao, Y., yu, Dai, ming, Q., Ma, G., shan, Zhang, feng, S., Cao, L., Ren, L., qun, Liu, feng, N., 2012. Erythropoietin attenuates cardiac dysfunction by increasing myocardial angiogenesis and inhibiting interstitial fibrosis in diabetic rats. Cardiovasc. Diabetol. 11, 1. https://doi.org/10.1186/1475-2840-11-105.

Lundby, C., Thomsen, J.J., Boushel, R., Koskolou, M., Warberg, J., Calbet, J.A.L., Robach, P., 2007. Erythropoietin treatment elevates haemoglobin concentration by increasing red cell volume and depressing plasma volume. J. Physiol. 578, 309–314. https://doi.org/10.1113/jphysiol.2006.122689.

Marinho, C.R.F., Bucci, D.Z., Dagli, M.L.Z., Bastos, K.R.B., Grisotto, M.G., Sardinha, L.R., Baptista, C.R.G.M., Gonçalves, C.P., D'Império Lima, M.R., Álvarez, J.M., 2004. Pathology affects different organs in two mouse strains chronically infected by A trypanosoma cruzi clone: a model for genetic studies of chagas' disease. Infect. Immun. 72, 2350–2357. https://doi.org/10.1128/IAI.72.4.2350-2357.2004.

Marsh, J.C., Boggs, D.R., Chervenick, P.A., Cartwright, G.E., Wintrobe, M.M., 1968. Factors influencing hematopoietic spleen colony formation in irradiated mice. IV. The effect of erythropoietic stimuli. J. Cell. Physiol. 71, 65–75. https://doi.org/10.1002/jcp.1040710109.

Marti, H.H., 2004. Erythropoietin and the hypoxic brain. J. Exp. Biol. 207, 3233–3242. https://doi.org/10.1242/jeb.01049.

Martinez, F., Perna, E., Perrone, S.V., Liprandi, A.S., 2019. Chagas disease and heart failure: an expanding issue worldwide. Eur. Cardiol. 14, 82–88. https://doi.org/10.15420/ecr.2018.30.2.

Mazzaccara, C., Labruna, G., Cito, G., Scarfò, M., De Felice, M., Pastore, L., Sacchetti, L., 2008. Age-related reference intervals of the main biochemical and hematological parameters in C57BL/6J, 129SV/EV and C3H/HeJ mouse strains. PLoS One 3, 4–10. https://doi.org/10.1371/journal.pone.0003772.

Medeiros, G.A., Silvério, J.C., Marino, A.P.M.P., Roffê, E., Vieira, V., Kroll-Palhares, K., Carvalho, C.E., Silva, A.A., Teixeira, M.M., Lannes-Vieira, J., 2009. Treatment of chronically Trypanosoma cruzi-infected mice with a CCR1/CCR5 antagonist (Met-RANTES) results in amelioration of cardiac tissue damage. Microb. Infect. 11, 264–273. https://doi.org/10.1016/j.micinf.2008.11.012.

Moore, E.M., Bellomo, R., Nichol, A.D., 2011. Erythropoietin as a novel brain and kidney protective agent. Anaesth. Intensive Care 39, 356–372. https://doi.org/10.1177/0310057x1103900306.

Moran, C.M., Thomson, A.J.W., Rog-Zielinska, E., Gray, G.A., 2013. High-resolution echocardiography in the assessment of cardiac physiology and disease in preclinical models. Exp. Physiol. 98, 629–644. https://doi.org/10.1113/expphysiol.2012.068577.

Morillo, C.A., Marin-Neto, J.A., Avezum, A., Sosa-Estani, S., Rassi, A., Rosas, F., Villena, E., Quiroz, R., Bonilla, R., Britto, C., Guhl, F., Velazquez, E., Bonilla, L., Meeks, B., Rao-Melacini, P., Pogue, J., Mattos, A., Lazdins, J., Rassi, A., Connolly, S. J., Yusuf, S., 2015. Randomized trial of benznidazole for chronic chagas' cardiomyopathy. N. Engl. J. Med. 373, 1295–1306. https://doi.org/10.1056/NEJMoa1507574.

Noyes, H.A., Alimohammadian, M.H., Agaba, M., Brass, A., Fuchs, H., Gailus-Durner, V., Hulme, H., Iraqi, F., Kemp, S., Rathkolb, B., Wolf, E., de Angelis, M.H., Roshandel, D., Naessens, J., 2009. Mechanisms controlling anaemia in Trypanosoma congolense infected mice. PLoS One 4. https://doi.org/10.1371/journal.pone.0005170.

Parada, H., Carrasco, H.A., Añez, N., Fuenmayor, C., Inglessis, I., 1997. Cardiac involvement is a constant finding in acute Chagas' disease: a clinical, parasitological and histopathological study. Int. J. Cardiol. 60, 49–54. https://doi.org/10.1016/S0167-5273(97)02952-5.

Pereira, I.R., Vilar-Pereira, G., da Silva, A.A., Lannes-Vieira, J., 2014. Severity of chronic experimental Chagas' heart disease parallels tumour necrosis factor and nitric oxide levels in the serum: models of mild and severe disease. Mem. Inst. Oswaldo Cruz 109, 289–298. https://doi.org/10.1590/0074-0276140033.

Pérez-Molina, J.A., Crespillo-Andújar, C., Bosch-Nicolau, P., Molina, I., 2021. Trypanocidal treatment of Chagas disease. Enferm. Infecc. Microbiol. Clín. 39, 458–470. https://doi.org/10.1016/j.eimc.2020.04.011.

Pinto, A.Y., das, N., da S Valente, S.A., da C Valente, V., 2004. Emerging acute Chagas disease in Amazonian Brazil: case reports with serious cardiac involvement. Braz. J. Infect. Dis. 8, 454–460. https://doi.org/10.1590/S1413-86702004000600010.

Pinto, A.Y.D.N., Valente, S.A., Valente, V.D.C., Ferreira, A.G., Coura, J.R., 2008. Fase aguda da doença de Chagas na Amazônia brasileira. Estudo de 233 casos do Pará, Amapá e Maranhão observados entre 1988 e 2005. Rev. Soc. Bras. Med. Trop. 41, 602–614. https://doi.org/10.1590/S0037-86822008000600011.

Prata, A., 2001. Clinical and epidemiological aspects of Chagas disease. Lancet Infect. Dis. 1, 92–100. https://doi.org/10.1016/S1473-3099(01)00065-2.

Puchulu, M.B., Arreche, N., Zotta, E., Donato, M., Ogonowski, N., Fellet, A., Balaszczuk, A.M., 2019. Erythropoietin improves cardiovascular function in adult rats after acute hemorrhage. J. Cardiovasc. Pharmacol. 73, 290–300. https://doi.org/10.1097/FJC.0000000000000666.

Qin, Y., Zhang, X., Yu, Y., Bian, X., Dong, S., 2013. Cardioprotective effect of erythropoietin on sepsisinduced myocardial injury in rats. World J. Emerg. Med. 4, 215–222. https://doi.org/10.5847/wjem.j.issn.1920-8642.2013.03.011.

Rassi, A., Marin-Neto, J.A., Rassi, A., 2017. Chronic chagas cardiomyopathy: a review of the main pathogenic mechanisms and the efficacy of aetiological treatment following the BENznidazole evaluation for interrupting trypanosomiasis (BENEFIT) trial. Mem. Inst. Oswaldo Cruz. https://doi.org/10.1590/0074-02760160334.

Ribeiro, M., Nitz, N., Santana, C., Moraes, A., Hagström, L., Andrade, R., Rios, A., Sousa, A., Dallago, B., Gurgel-Gonçalves, R., Hecht, M., 2016. Sexual transmission of Trypanosoma cruzi in murine model. Exp. Parasitol. 162 https://doi.org/10.1016/j.exppara.2015.12.017.

Ribeiro, V., Dias, N., Paiva, T., Hagström-Bex, L., Nitz, N., Pratesi, R., Hecht, M., 2020. Current trends in the pharmacological management of Chagas disease. Int. J. Parasitol. Drugs Drug Resist. 12, 7–17. https://doi.org/10.1016/j.ijpddr.2019.11.004.

Riksen, N.P., Hausenloy, D.J., Yellon, D.M., 2008. Erythropoietin: ready for prime-time cardioprotection. Trends Pharmacol. Sci. 29, 258–267. https://doi.org/10.1016/j.tips.2008.02.002.

Rodrigues-dos-Santos, Í., Melo, M.F., de Castro, L., Hasslocher-Moreno, A.M., do Brasil, P.E.A.A., Silvestre de Sousa, A., Britto, C., Moreira, O.C., 2018. Exploring the parasite load and molecular diversity of Trypanosoma cruzi in patients with chronic Chagas disease from different regions of Brazil. PLoS Neglected Trop. Dis. 12 https://doi.org/10.1371/journal.pntd.0006939.

Roth, D., Swaney, J., Dalton, N., Gilpin, E., Ross Jr., J., 2002. Impact of anesthesia on cardiac function during echocardiography in mice. Am. J. Physiol. Heart Circ. Physiol. 282, H2134–H2140. https://doi.org/10.1152/ajpheart.00845.2001.

Rottman, J.N., Ni, G., Khoo, M., Wang, Z., Zhang, W., Anderson, M.E., Madu, E.C., 2003. Temporal changes in ventricular function assessed echocardiographically in conscious and anesthetized mice. J. Am. Soc. Echocardiogr. 16, 1150–1157. https://doi.org/10.1067/S0894-7317(03)00471-1.

Rui, T., Feng, Q., Lei, M., Peng, T., Zhang, J., Xu, M., Dale Abel, E., Xenocostas, A., Kvietys, P.R., 2005. Erythropoietin prevents the acute myocardial inflammatory response induced by ischemia/reperfusion via induction of AP-1. Cardiovasc. Res. 65, 719–727. https://doi.org/10.1016/j.cardiores.2004.11.019.

Ruijter, J.M., Ruiz Villalba, A., Hellemans, J., Untergasser, A., van den Hoff, M.J.B., 2015. Removal of between-run variation in a multi-plate qPCR experiment. Biomol. Detect. Quantif. 5, 10–14. https://doi.org/10.1016/j.bdq.2015.07.001.

Sanchis-Gomar, F., Garcia-Gimenez, J.L., Pareja-Galeano, H., Romagnoli, M., Perez-Quilis, C., Lippi, G., 2014. Erythropoietin and the heart: physiological effects and the therapeutic perspective. Int. J. Cardiol. 171, 116–125. https://doi.org/10.1016/j.ijcard.2013.12.011.

Santacruz, D., Rosas, F., Hardy, C.A., Ospina, D., Rosas, A.N., Camargo, J.M., Bermúdez, J.J., Betancourt, J.F., Velasco, V.M., González, M.D., 2021. Advanced management of ventricular arrhythmias in chronic Chagas cardiomyopathy. Hear. Rhythm O2 2, 807–818. https://doi.org/10.1016/j.hroo.2021.10.010.

Santos, Lilian da Silva, Torres, Rosália Morais, Machado-de-Assis, Girley Francisco, Bahia, Maria Terezinha, Martins, Helen Rodrigues, Teixeira-Carvalho, Andréa, Coelho-dos-Reis, Jordana Grazziela Alves, Albajar-Viñas, Pedro, Martins-Filho, Olindo Assis, de Lana, Marta, 2012. In-house ELISA method to analyze anti-*Trypanosoma cruzi* IgG reactivity for differential diagnosis and evaluation of Chagas disease morbidity. Rev. Soc. Bras. Med. Trop. 45 (1), 35–44. doi:10.1590/s0037-86822012000100008.

Scarim, C.B., de Andrade, C.R., da Rosa, J.A., dos Santos, J.L., Chin, C.M., 2018. Hydroxymethylnitrofurazone treatment in indeterminate form of chronic Chagas disease: reduced intensity of tissue parasitism and inflammation—a histopathological study. Int. J. Exp. Pathol. 99, 236–248. https://doi.org/10.1111/iep.12289.

Silberstein, E., Serna, C., Fragoso, S.P., Nagarkatti, R., Debrabant, A., 2018. A novel nanoluciferase-based system to monitor Trypanosoma cruzi infection in mice by bioluminescence imaging. PLoS One 13, 1–21. https://doi.org/10.1371/journal.pone.0195879.

Silva, E., Da, R., Passos, H., Ferri, M.B., Francisco, L., 2008. Sepsis: from bench to bedside. Clinics 63, 109–120. https://doi.org/10.1590/s1807-59322008000100019.

Silverio, J.C., Pereira, I.R., Cipitelli, M. da C., Vinagre, N.F., Rodrigues, M.M., Gazzinelli, R.T., Lannes-Vieira, J., 2012. CD8+ T-cells expressing interferon gamma or perforin play antagonistic roles in heart injury in experimental trypanosoma cruzi-elicited cardiomyopathy. PLoS Pathog. 8 https://doi.org/10.1371/journal.ppat.1002645.

Smith, K.J., Bleyer, A.J., Little, W.C., Sane, D.C., 2003. The cardiovascular effects of erythropoietin. Cardiovasc. Res. 59, 538–548. https://doi.org/10.1016/S0008-6363(03)00468-1.

Soares, R.C.O., Cristiano, S.-S., Franzói-de-Moraes, S., Batista, M.R., Kwabara, H.N., Sousa, A.M.R., Moreira, N.M., Gomes, M.L., Araújo, S.M., 2012. Experimental infection with trypanosoma cruzi in mice : influence of exercise. Rev. Bras. Med. Esporte. 18, 51–57.

Sølling, C., 2012. Organ-protective and immunomodulatory effects of erythropoietin - an update on recent clinical trials. Basic Clin. Pharmacol. Toxicol. 110, 113–121. https://doi.org/10.1111/j.1742-7843.2011.00820.x.

Stypmann, J., Engelen, M.A., Epping, C., van Rijen, H.V.M., Milberg, P., Bruch, C., Breithardt, G., Tiemann, K., Eckardt, L., 2006. Age and gender related reference

values for transthoracic Doppler-echocardiography in the anesthetized CD1 mouse. Int. J. Cardiovasc. Imag. 22, 353–362. https://doi.org/10.1007/s10554-005-9052-9.

Stypmann, J., Engelen, M.A., Troatz, C., Rothenburger, M., Eckardt, L., Tiemann, K., 2009. Echocardiographic assessment of global left ventricular function in mice. Lab. Anim. 43, 127–137. https://doi.org/10.1258/la.2007.06001e.

Stypmann, J., Gläser, K., Roth, W., Tobin, D.J., Petermann, I., Matthias, R., Mönnig, G., Haverkamp, W., Breithardt, G., Schmahl, W., Peters, C., Reinheckel, T., 2002. Dilated cardiomyopathy in mice deficient for the lysosomal cysteine peptidase cathepsin L. Proc. Natl. Acad. Sci. U. S. A 99, 6234–6239. https://doi.org/10.1073/pnas.092637699.

Suresh, S., Rajvanshi, P.K., Noguchi, C.T., 2020. The many facets of erythropoietin physiologic and metabolic response. Front. Physiol. 10, 1–20. https://doi.org/10.3389/fphys.2019.01534.

Suzuki, T., Ueta, Y.Y., Inoue, N., Xuan, X., Saitoh, H., Suzuki, H., 2006. Beneficial effect of erythropoietin administration on murine infection with Trypanosoma congolense. Am. J. Trop. Med. Hyg. 74, 1020–1025. https://doi.org/10.4269/ajtmh.2006.74.1020.

Syed, F., Diwan, A., Hahn, H.S., 2005. Murine echocardiography: a practical approach for phenotyping genetically manipulated and surgically modeled mice. J. Am. Soc. Echocardiogr. 18, 982–990. https://doi.org/10.1016/j.echo.2005.05.001.

Takawale, A., Fan, D., Basu, R., Shen, M., Parajuli, N., Wang, W., Wang, X., Oudit, G.Y., Kassiri, Z., 2014. Myocardial recovery from ischemia-reperfusion is compromised in the absence of tissue inhibitor of metalloproteinase 4. Circ. Hear. Fail 7, 652–662. https://doi.org/10.1161/CIRCHEARTFAILURE.114.001113.

Tangri, N., Stevens, L.A., Griffith, J., Tighiouart, H., Djurdjev, O., Naimark, D., Levin, A., Levey, A.S., 2011. A predictive model for progression of chronic kidney disease to kidney failure. JAMA, J. Am. Med. Assoc. 305, 1553–1559. https://doi.org/10.1001/jama.2011.451.

Teixeira, A.R.L., Hecht, M.M., Guimaro, M.C., Sousa, A.O., Nitz, N., 2011. Pathogenesis of chagas' disease: parasite persistence and autoimmunity. Clin. Microbiol. Rev. 24, 592–630. https://doi.org/10.1128/CMR.00063-10.

Tramontano, A.F., Muniyappa, R., Black, A.D., Blendea, M.C., Cohen, I., Deng, L., Sowers, J.R., Cutaia, M.V., El-Sherif, N., 2003. Erythropoietin protects cardiac myocytes from hypoxia-induced apoptosis through an Akt-dependent pathway. Biochem. Biophys. Res. Commun. 308, 990–994. https://doi.org/10.1016/S0006-291X(03)01503-1.

Villalba-Alemán, E., Justinico, D.L., Sarandy, M.M., Novaes, R.D., Freitas, M.B., Gonçalves, R.V., 2018. Haematological alterations in non-human hosts infected with Trypanosoma cruzi: a systematic review. Parasitology 1–19. https://doi.org/10.1017/S0031182018001294.

Vinhas, M., Araújo, A.C., Ribeiro, S., Rosário, L.B., Belo, J.A., 2013. Transthoracic echocardiography reference values in juvenile and adult 129/Sv mice. Cardiovasc. Ultrasound 11, 1–10. https://doi.org/10.1186/1476-7120-11-12.

Wakhloo, D., Scharkowski, F., Curto, Y., Javed Butt, U., Bansal, V., Steixner-Kumar, A.A., Wüstefeld, L., Rajput, A., Arinrad, S., Zillmann, M.R., Seelbach, A., Hassouna, I., Schneider, K., Qadir Ibrahim, A., Werner, H.B., Martens, H., Miskowiak, K., Wojcik, S.M., Bonn, S., Nacher, J., Nave, K.A., Ehrenreich, H., 2020. Functional hypoxia drives neuroplasticity and neurogenesis via brain erythropoietin. Nat. Commun. 11, 1–12. https://doi.org/10.1038/s41467-020-15041-1.

Wang, J., Hayashi, Y., Yokota, A., Xu, Z., Zhang, Y., Huang, R., Yan, X., Liu, H., Ma, L., Azam, M., Bridges, J.P., Cancelas, J.A., Kalfa, T.A., An, X., Xiao, Z., Huang, G., 2018. Expansion of EPOR-negative macrophages besides erythroblasts by elevated EPOR signaling in erythrocytosis mouse models. Haematologica 103, 69–79. https://doi.org/10.3324/haematol.2017.172775.

Wesley, M., Moraes, A., de C Rosa, A., Carvalho, J.L., Shiroma, T., Vital, T., Dias, N., de Carvalho, B., Rabello, D.D.A., Borges, T.K.D.S., Dallago, B., Nitz, N., Hagström, L., Hecht, M., 2019. Correlation of parasite burden, kdna integration, autoreactive antibodies, and cytokine pattern in the pathophysiology of chagas disease. Front. Microbiol. 10 https://doi.org/10.3389/fmicb.2019.01856.

WHO, 2019. Media centre: chagas disease (American trypanosomiasis). Fact sheet 1–6. https://doi.org/10.1002/0471743984.vse1619.

Wincker, P., Britto, C., Pereira, J.B., Cardoso, M.A., Oelemann, W., Morel, C.M., 1994. Use of a simplified polymerase chain reaction procedure to detect Trypanosoma cruzi in blood samples from chronic chagasic patients in a rural endemic area. Am. J. Trop. Med. Hyg. 51, 771–777. https://doi.org/10.4269/ajtmh.1994.51.771.

Wright, G.L., Hanlon, P., Amin, K., Steenbergen, C., Murphy, E., Arcasoy, M.O., 2004. Erythropoietin receptor expression in adult rat cardiomyocytes is associated with an acute cardioprotective effect for recombinant erythropoietin during ischemia-reperfusion injury. Faseb. J. 18, 1031–1033. https://doi.org/10.1096/fj.03-1289fje.

Xu, H., van Deel, E.D., Johnson, M.R., Opić, P., Herbert, B.R., Moltzer, E., Sooranna, S.R., van Beusekom, H., Zang, W.F., Duncker, D.J., Roos-Hesselink, J.W., 2016. Pregnancy mitigates cardiac pathology in a mouse model of left ventricular pressure overload. Am. J. Physiol. Heart Circ. Physiol. 311, H807–H814. https://doi.org/10.1152/ajpheart.00056.2016.

Xue, H., Li, J., Xie, H., Wang, Y., 2018. Review of drug repositioning approaches and resources. Int. J. Biol. Sci. 14, 1232–1244. https://doi.org/10.7150/ijbs.24612.

Yang, X.P., Liu, Y.H., Rhaleb, N.E., Kurihara, N., Kim, H.E., Carretero, O.A., 1999. Echocardiographic assessment of cardiac function in conscious and anesthetized mice. Am. J. Physiol. Heart Circ. Physiol. 277 https://doi.org/10.1152/ajpheart.1999.277.5.h1967.

Zauza, Patrícia Lago, Borges-Pereira, José, 2001. Sera levels of anti-*Trypanosoma cruzi* IgG in the course of chronic chagasic cardiopathy in 10 years. Rev. Soc. Bras. Med. Trop. 34 (5), 399–405. doi:10.1590/s0037-86822001000500001.

Zhou, X., Hansson, G.K., 2004. Effect of sex and age on serum biochemical reference ranges in C57BL/6J mice. Comp. Med. 54, 176–178.

Zingales, B., Andrade, S., Briones, M.R.S., Campbell, D., Chiari, E., Fernandes, O., Guhl, F., Lages-Silva, E., Macedo, C., Miles, M.A., Romanha, A.J., Sturm, N.R., Tibayrenc, M., Schijman, A.G., 2009. A new consensus for Trypanosoma cruzi intraspecific nomenclature: second revision meeting recommends TcI to TcVI. Mem. Inst. Oswaldo Cruz 104, 1051–1054.